

POLITECNICO DI MILANO
School of Industrial and Information Engineering
Master of Science in Chemical Engineering



POLITECNICO
MILANO 1863

Aqueous phase reforming of renewables for hydrogen production in presence of supported platinum and palladium catalysts.

Supervisors:

Prof. Carlo Giorgio Visconti – Politecnico di Milano

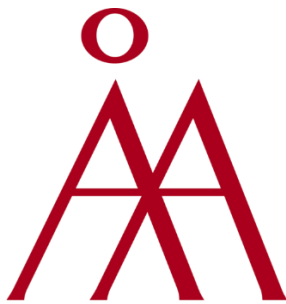
Prof. Dmitry Yu. Murzin – Åbo Akademi

Master Candidate:

Matias Ignacio Alvear Cabezón

897598

Academic Year 2018 - 2019



Project developed in:

Laboratory of Industrial Chemistry and Reaction Engineering

Department of Chemical Engineering

Åbo Akademi University

Contents

Abstract	12
Acknowledgements	14
1 Introduction:	16
State of art:.....	20
1.1.1 Ethylene Glycol:.....	20
1.1.2 Glycerol:.....	21
1.1.3 Erythritol:.....	22
1.1.4 Xylitol:	22
1.1.5 Xylose:.....	22
1.1.6 Sorbitol:.....	23
2 Experimental part.....	25
2.1.1 Set-up	25
2.1.2 Micro gas chromatograph (micro-GC) calibration:	26
2.1.3 High pressure liquid chromatograph calibration.....	26
2.1.4 Experiments:.....	26
2.1.5 Calculations of conversion, selectivities and yields.....	28
2.1.6 Results:.....	28
2.2 Substrate effect	31
2.2.1 Ethylene Glycol.....	31
2.2.2 Glycerol.....	32
2.2.3 Erythritol.....	34
2.2.4 Xylitol	35
2.2.5 Xylose.....	36
2.2.6 Sorbitol	38
2.3 Alkane behavior.....	40
2.3.1 Ethylene glycol.....	40
2.3.2 Glycerol:.....	41
2.3.3 Erythritol:.....	41
2.3.4 Xylitol	42
2.3.5 Xylose.....	43

2.3.6	Sorbitol	43
2.4	Liquid phase composition	45
2.4.1	Ethylene glycol:.....	45
2.4.2	Glycerol:.....	46
2.4.3	Erythritol:.....	47
2.4.4	Xylitol:	47
2.4.5	Xylose:.....	48
2.4.6	Sorbitol:.....	49
2.5	Liquid - Gas carbon distribution:.....	50
2.5.1	Ethylene glycol:.....	50
2.5.2	Glycerol:.....	51
2.5.3	Erythritol:.....	52
2.5.4	Xylitol:	53
2.5.5	Xylose:.....	54
2.5.6	Sorbitol:.....	55
2.6	Carbon balance:.....	57
2.6.1	Ethylene glycol:.....	57
2.6.2	Glycerol:.....	58
2.6.3	Erythritol:.....	58
2.6.4	Xylitol:	59
2.6.5	Xylose:.....	60
2.6.6	Sorbitol:.....	60
2.7	Effect of catalyst composition	62
2.8	Discussion	65
3	Kinetic modeling of ethylene glycol APR.....	70
3.1	Mathematical modeling	70
3.2	Experiments	71
3.3	Results and discussion:.....	72
4	Conclusions:	76
5	References	78
6	Appendix A	81
7	Appendix B	82

8 Appendix C 83
9 Appendix D 87

List of Figures:

Figure 1 Reaction pathways for ethylene glycol aqueous phase reforming [15]. ...	20
Figure 2 Reaction pathways for glycerol aqueous phase reforming [16].	21
Figure 3 Xylitol APR process flow diagram [23].	22
Figure 4 Aqueous phase reforming of sorbitol: Main transformation pathways [24].	23
Figure 5 Experimental set-up for aqueous phase reforming.	25
Figure 6 Conversion for ethylene glycol aqueous phase reforming.	31
Figure 7 Selectivity graph of ethylene glycol APR.	32
Figure 8 Conversion for glycerol aqueous phase reforming.	33
Figure 9 Selectivity graph of glycerol APR.	33
Figure 10 Conversion for erythritol aqueous phase reforming.	34
Figure 11 Selectivity graph of erythritol APR.	35
Figure 12 Conversion for xylitol aqueous phase reforming.	35
Figure 13 Selectivity graph of xylitol APR.	36
Figure 14 Conversion for xylose aqueous phase reforming.	37
Figure 15 Selectivity graph of xylose APR.	37
Figure 16 Conversion for sorbitol aqueous phase reforming.	38
Figure 17 Selectivity graph of sorbitol APR.	39
Figure 18 Alkane selectivity for ethylene glycol APR.	40
Figure 19 Alkane selectivity for glycerol APR.	41
Figure 20 Alkane selectivity for erythritol APR.	42
Figure 21 Alkane selectivity for xylitol APR.	42
Figure 22 Alkane selectivity for xylose APR.	43
Figure 23 Alkane selectivity for sorbitol APR.	44
Figure 24 Liquid distribution in ethylene glycol APR.	46
Figure 25 Liquid distribution in glycerol APR.	46
Figure 26 Liquid distribution in erythritol APR.	47
Figure 27 Liquid distribution in xylitol APR.	48
Figure 28 Liquid phase distribution of products in xylose APR.	48
Figure 29 Distribution of the liquid phase products in the APR of sorbitol.	49
Figure 30 Distribution of (a) gas phase and (b) liquid phase products in ethylene glycol APR.	51
Figure 31 Distribution of (a) gas phase and (b) liquid phase products in glycerol APR.	52
Figure 32 Distribution of (a) gas phase and (b) liquid phase products in erythritol APR.	53
Figure 33 Distribution of (a) gas phase and (b) liquid phase products in xylitol APR.	54
Figure 34 Distribution of (a) gas phase and (b) liquid phase products in xylose APR.	55

Figure 35 Distribution of (a) gas phase and (b) liquid phase products in sorbitol APR.	56
Figure 36 Carbon balance in ethylene glycol APR.	57
Figure 37 Carbon balance in glycerol APR.....	58
Figure 38 Carbon balance in erythritol APR.	59
Figure 39 Carbon balance in xylitol APR.	59
Figure 40 Carbon balance in xylose APR.	60
Figure 41 Carbon balance in sorbitol APR.	61
Figure 42 Yield of products in xylose with formic acid APR over different catalysts.	63
Figure 43 Yield of alkanes in APR of xylose with formic acid over different catalysts.	64
Figure 44 An example of C-O bond hydrogenolysis.	65
Figure 45 An example of aldol condensation.....	66
Figure 46 An example of dehydration reaction.	66
Figure 47 Xylose hydro-dehydroxylation.	66
Figure 48 An example of acid formation.	66
Figure 49 An example of decarbonylation reaction.	67
Figure 50 Example of retro-aldol reaction.....	67
Figure 51 Aqueous phase reforming of ethylene glycol: main pathways selected for mathematical model.	70
Figure 52 Ethylene glycol APR model vs experimental data.	73
Figure 53 Hydrogen production model vs experimental data.	73
Figure 54 Carbon dioxide production model vs experimental data.	74
Figure 55 Methanol production model vs experimental data.	74
Figure 56 Ethylene glycol molar flow at the reactor outlet.	75
Figure A1 Complete reaction scheme of ethylene glycol APR.	81
Figure B1 Reaction path tested for ethylene glycol modeling.....	82
Figure C1 Conversion vs Flow at 200°C.....	83
Figure C2 Conversion vs Flow at 225°C.....	83
Figure C3 Conversion vs Flow at 250°C.....	84
Figure D1 Ea1 vs k1.....	87
Figure D2 Ea2 vs k2.....	88
Figure D3 Ea3 vs k3.....	88
Figure D4 Sensitivity by parameter.	89

List of Tables

Table 1 Gases calibrated in the micro GC.....	26
Table 2 Substrates calibrated in the HPLC.....	26
Table 3 Substrates.	27
Table 4 Catalyst tested.....	62
Table 5 Conditions tested during the mechanism experiment	72
Table 6 Reaction constants and activation energies.	72
Table 7 Data used for ethylene glycol modeling.	85
Table 8 Parameters with errors.	87

Abstract

The aqueous phase reforming (APR) of five polyols and one sugar was studied over Pt/Pd catalysts supported on mesoporous carbon. The temperatures were between 175°C to 225°C and addition of formic acid was studied for potential industrial application.

During the analyses 45 compounds were identified and quantified (17 in the gas phase and 28 in the liquid phase). As a result the carbon identification was complete for most of the substrates. The C5 compounds (xylitol and xylose) did not have a complete carbon balance as a consequence of complex furans chemistry.

The polyols displayed an elevated production of hydrogen and carbon dioxide at all conditions, but it could be even improved by temperature increase and addition of formic acid. The sugar (xylose) shows changes in the hydrogen selectivity with the conditions increasing the alkane production with temperature and formic acid addition.

According to the results the retro-aldol reaction it is the main route for C-C bond cleavage, which is promoted by dehydrogenation or dehydration reactions. The presence of decarbonylation was observed but to lower extent and it could have been related to alkane production.

Experiments with different catalyst composition were done. Large changes in the gas products formation were observed. The best ratio for Pt and Pd was 2:1 respectively, because it gave an increase in selectivity to hydrogen and stopped the carbon monoxide production in most of the conditions tested.

The ethylene glycol APR reaction path was condensed to the most abundant products for the model generation. The final kinetic model displayed a 99.56% of correspondence with the experimental data. The reactor behavior was described using a plug flow model.

Acknowledgements

I would like to express my deep gratitude to Prof Dmitry Murzin, for his patient guidance, enthusiastic encouragement and useful critiques of this project. His willingness to give his time so generously has been very much appreciated during all my stay in Åbo Akademi.

My special thanks are extended to Prof. Carlo Visconti for accepting me as his master thesis student, for being the supervisor of this work at Politecnico di Milano and for his support even from distance.

I would also like to thank Atte Aho, for his advice and assistance in keeping my progress. My grateful thanks are also extended to Johan Wärnå for his help in doing the ethylene glycol model and to Kari Eränen, who helped me to repair my setup countless times.

I wish to thank my parents and my brothers for their support, encouragement throughout my studies and to be great role models for my life.

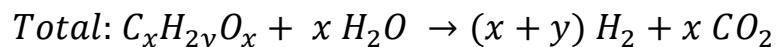
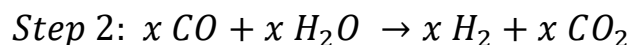
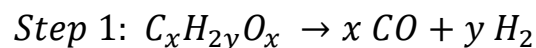
Finally, Special thanks should be given to my girlfriend Alli and all my friends and people who made this journey unforgettable. Special thanks are given to Boguslaw, Los Venenosos and El frenillo de acero.

1 Introduction:

During the last decades an important increase in the energy demand has been noticed followed by the massive utilization of fossil fuels in the developing countries. This makes a sustainable evolution of our society impossible without the utilization of energy from renewable sources including biomass, solar, wind, hydroelectric power etc. During the coming years the renewable energy is going to grow in diverse ways as an answer to different problems that have to be solved in each of the sources. In the case of biomass, conversion into fuels is a challenge that requires time to be implemented in industry. Production of hydrogen for fuel cells and other industrial applications from biomass is a part of the quest for a viable future.

Nowadays the main source of hydrogen production is methane steam reforming. However, this process has a high energy consumption and is based on the fossil feedstock. This method is energy demanding because the reaction is endothermic requiring high temperature and is not sustainable due to CO₂ release to atmosphere. As an answer to these problems in 2002 Dumesic et al. developed a single step process for production of renewable hydrogen at low temperature using heterogeneous catalysis known as the aqueous phase reforming [1].

The Aqueous Phase Reforming (APR) process is a new path for production of hydrogen and carbon dioxide from biomass derived oxygenated compounds. This process is composed of two steps. In the first one, the substrate is transformed into H₂ and CO. This conversion happens on a metal supported catalyst at low temperature (175 - 250 °C) and high pressure (20 – 40 atm). The operational conditions make the water gas shift reaction possible which constitutes the second step of the process. In this reaction carbon monoxide reacts with water, generating hydrogen. The overall scheme is thus:



The aqueous phase reforming have multiple advantages such as:

- Neutral greenhouse emissions [2], because the raw material is biomass, consequently all CO₂ produced have been already captured from the atmosphere.

- Compared to steam reforming, APR allows a reduction of energy consumption by elimination of a need to vaporize water and the oxygenated hydrocarbons.
- Water is used as a solvent and also as a reactant being converted into additional hydrogen via the water gas shift reaction because the APR occurs at temperatures and pressures where the reaction is favorable [3].
- Finally, the reactants are not flammable and non-toxic. Hence the process is inherently safe.

APR is therefore becoming an interesting path for production of hydrogen, however further research is required to solve remaining challenges. The catalyst stability and the yield are the main ones. Nevertheless APR is a highly adjustable process, where activity and selectivity can be modified with different parameters such as nature of the catalyst (metal components and support material), reaction conditions and the cluster size.

Many metals are active in aqueous phase reforming. A broad metal screening was performed for supported catalysts [3]. Platinum was shown to be highly active and selective for hydrogen production, which can be even further improved by the addition of a second transition metal [4]. Certain attempts were made to find a replacement of this expensive metal, however, so far researchers were only partially successful because of stability issues as sintering, oxidation and metal leaching [5, 6].

The process could be structure sensitive, due to higher activity in the presence of larger cluster sizes [7]. Nevertheless hydrogen selectivity increases with the particle size while the reaction rates were not improved for a platinum catalyst [8].

The reaction pathway depends strongly on the support. Polarity, hydrophobicity and specially acidity play an essential role in the final product distribution [9]. Oxide supports with a higher electron donating character evidence an increase in activity and selectivity to hydrogen [10].

The APR shows a pH influence on the distribution of the reaction products over some catalysts. Basic conditions tend to promote hydrogen formation, leading however, to catalyst deactivation. A higher carbon chain length in the reactants promotes a higher alkane selectivity [11].

Hydrogen has an important role in selectivity in particular to alkanes. Therefore it is imperative to have a control on the hydrogen partial pressures to decrease this effect [12]. The increase of hydrogen and carbon dioxide partial pressures drives the water gas shift reaction in the reverse direction leading to carbon monoxide coverage of the metal surface [13].

Certainly the aqueous phase reforming is a complex process which is still under development and all of these tunable variables controlled in the right way promise a bright future for this technology.

State of art:

The aim of this chapter is to report work done with the different substrates which were used in this project related to aqueous phase reforming. These substrates were ethylene glycol, glycerol, erythritol, xylitol, xylose and sorbitol. It should be noted that the amount of work in the literature for every substrate is different. Moreover the aqueous phase reforming until now does not have industrial applications therefore the literature shows exploratory results.

1.1.1 Ethylene Glycol:

The research on ethylene glycol is broad in conditions, metals and supports. Shabaker and Dumesic [14, 15] in a broad work with this substrate found that the highest catalytic activity was exhibited by supported platinum catalyst at 500 K. In terms of pressure the system was always 3 bar over the steam pressure of the solution. In addition they proposed a reaction network and later performed kinetic modeling.

Figure 1 shows the kinetic pathways for ethylene glycol at 500 K over Pt/Al₂O₃ proposed by Dumesic et al. [15]. In there the alkane production was related to dehydrated compounds. Moreover production of acetic acid during ethylene glycol aqueous phase reforming was reported in [14]. This product can play a role in the increase of selectivity to alkanes too [15].

Methanol is decomposed in order to produce more carbon dioxide and hydrogen and also is included in condensations to ethylene glycol. Nevertheless the dehydrogenation reaction was considered as hydrogen and carbon dioxide promoters in this model.

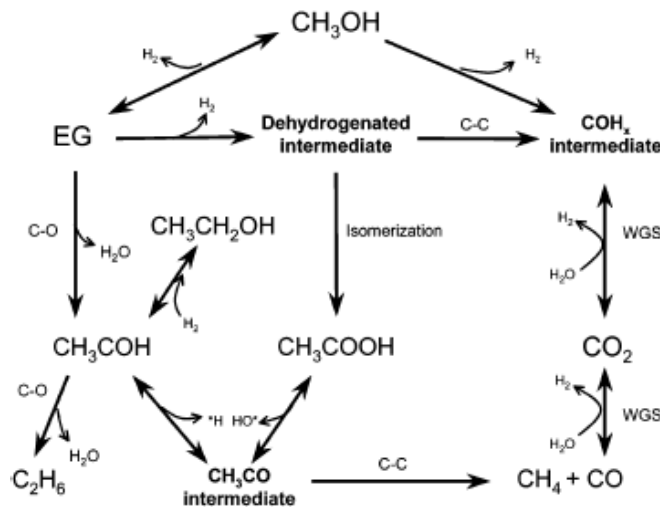


Figure 1 Reaction pathways for ethylene glycol aqueous phase reforming [15].

1.1.2 Glycerol:

The glycerol aqueous phase reforming generated a lot of interest in the last decade. A broad range of catalysts and conditions were tested. Additionally many reaction pathways were proposed. Luo et al. proposed one of the most complete reaction pathways with a clear distinction between the liquid and gas reactions [16]. Figure 2 presents the reaction pathway for glycerol at 500 K over Pt/Al₂O₃ proposed by Luo et al. It is important to recognize the condensation by dehydration of glycerol and separation between the gas and liquid phase pathways. Nevertheless the C2 intermediates produced after the glycerol C-C cleavage generate ethanol and acetic acid promoting alkane formation in the ethylene glycol aqueous phase reforming. However testing different catalysts and supports demonstrated a modification of the reaction pathways with the catalyst [17, 18, 19].

Luo et al. discovered structural changes of alumina (Al₂O₃) to bohemite (Al₂(OOH)₂) in the aqueous phase reforming under hydrothermal conditions. In addition Godina et al. investigating C3 compounds with a different number of hydroxyl groups on a Pt/C catalyst found a dependence of the number of hydroxyl groups in the molecules on the activity and selectivity to alkanes. On the other hand, a lack of methane in the gas phase suggests absence of methanation over platinum supported on carbon [17].

Addition of a second metal was tested with Re over Pt/C catalyst showing an increase in the hydrogen selectivity and a larger gasification of carbon. This is due to an increase in the acidity by Re addition [19].

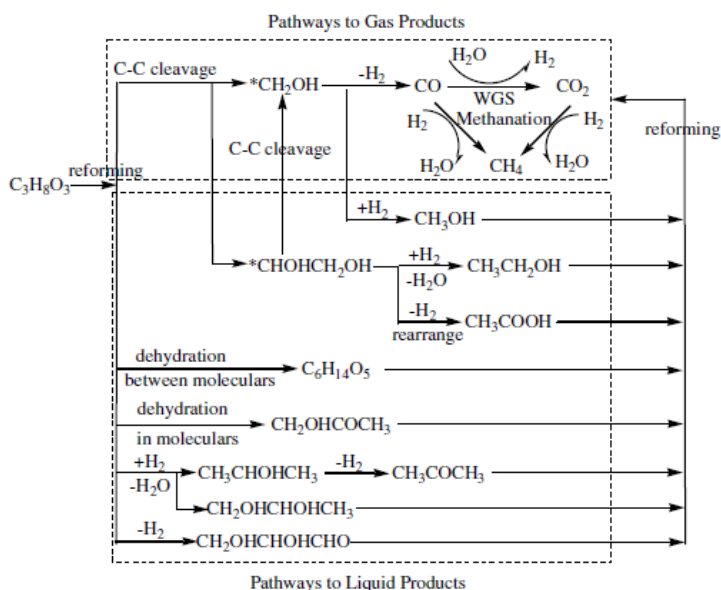


Figure 2 Reaction pathways for glycerol aqueous phase reforming [16].

1.1.3 Erythritol:

This substrate was practically not investigated being mentioned only as an intermediate of aqueous phase reforming of other polyols.

1.1.4 Xylitol:

Aqueous phase reforming of xylitol has been reported in several publications. Kirilin et al. reported a detailed screening of this substrate using mono- and bimetallic catalysts and different supports [20, 21, 22]. Where platinum displayed the best hydrogen selectivity in the mono metallic catalyst. Kirilin et al. and Godina et al. exploring addition of Re as a second metal found that because of acidity changes the hydrogen selectivity was improved [22, 20]. On the other hand the support shows different stability during long term experiments making the carbon based catalysts a good option as they are stable under hydrothermal conditions [21].

Murzin et al. studied the aqueous phase reforming of xylitol over Pt/C catalyst at 225°C and 30 bar with different residence times. During the tests formation of CO was negligible and C3 was presented in the highest amounts among alkanes. Kinetic modeling and process design was done by Murzin et al. being until now the only example of a complete integration of the aqueous phase reforming of xylitol in a process flow diagram [23]. The kinetic model was able to account for liquid products and for the gas phase byproduct (alkanes) could be used as a fuel for the reactor heating [23].

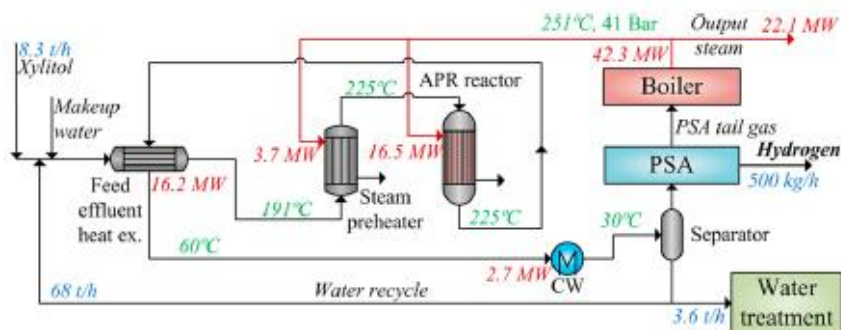


Figure 3 Xylitol APR process flow diagram [23].

The xylitol process diagram (Figure 3) presents low complexity and the hydrogen purification via pressure swing adsorption. In addition the boiler energy is fully covered by the tail gas. The effluent from the reactor is used for energy recuperation and later is cooled to 30°C for an efficient separation.

1.1.5 Xylose:

No data are available for aqueous phase reforming of xylose. Nevertheless it is mentioned as an intermediate in the reaction pathway of xylitol and sorbitol to hydrogen and alkanes.

1.1.6 Sorbitol:

There are many studies on the aqueous phase reforming of sorbitol. Being the liquid phase hard to analyze. Because during the product identification, over 260 compounds were detected with 50 of them being the major ones. Moreover the reaction conditions had an influence on the liquid and gas phase products [25].

Godina et al. investigated the effect of chirality in the aqueous phase reforming of C6 polyols (galactitol and sorbitol). Both demonstrated similar behavior during the initial stages of the APR and the selectivity for hydrogen and alkanes was almost the same. This means that substrates with different chirality can be used as mixtures [26].

As a result of a good product identification a better understanding of the system was achieved [25, 26] making possible to define the reaction pathways of sorbitol.

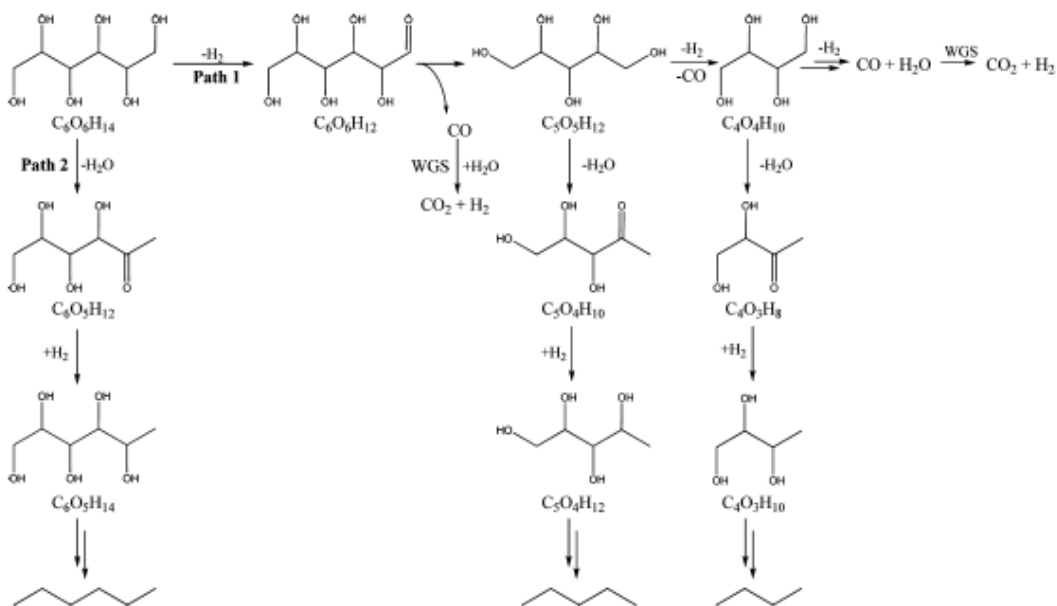


Figure 4 Aqueous phase reforming of sorbitol: Main transformation pathways [24].

The main reaction pathways identified by Kirilin et al. are present in Figure 4. The sorbitol transformation goes through dehydrogenations followed by decarbonylation to smaller polyols until the entire molecule is transformed to CO and H₂. However, every step can induce alkane production via hydrogenolysis of the C-O bond.

Kinetic modeling of sorbitol aqueous phase reforming done by Kirilin et al. was made for the experimental data generated at 225°C and 29.3 bar. The model gave a good correspondence between the experiments and calculations. Nevertheless the model can be further improved by taking into account other sorbitol reaction pathways [24].

2 Experimental part

The aim of this chapter is to report the experiment work done during this study. During this experiments six substrates were tested. Moreover the different phases were quantified and analyzed.

2.1.1 Set-up

Figure 5 presents the setup which was used. This system contains a trickle bed reactor fed with nitrogen containing 1% helium and a feed of the liquid phase i.e the liquid substrate solution. The reactor was of 50 cm length and 4.6 mm of internal diameter. The catalyst was diluted in glass beads in a proportion of 1:6 respectively. The liquid phase is pumped by a chromatography pump and the gas phase through the flow controller MFC-1. Downstream the reactor the pressure is controlled by a membrane pressure controller Equilibar. After the pressure controller (PC-1) located downstream the reactor the gas liquid separator is placed, operating at room temperature. In the separator the liquid sample is collected to be analyzed offline by the liquid chromatography. The gas phase goes through a condenser at -5°C to prevent clogging the micro gas chromatograph. After the condenser most of the gas phase goes to the vent and the rest is routed the micro-GC for the on-line analysis of the gas stream.

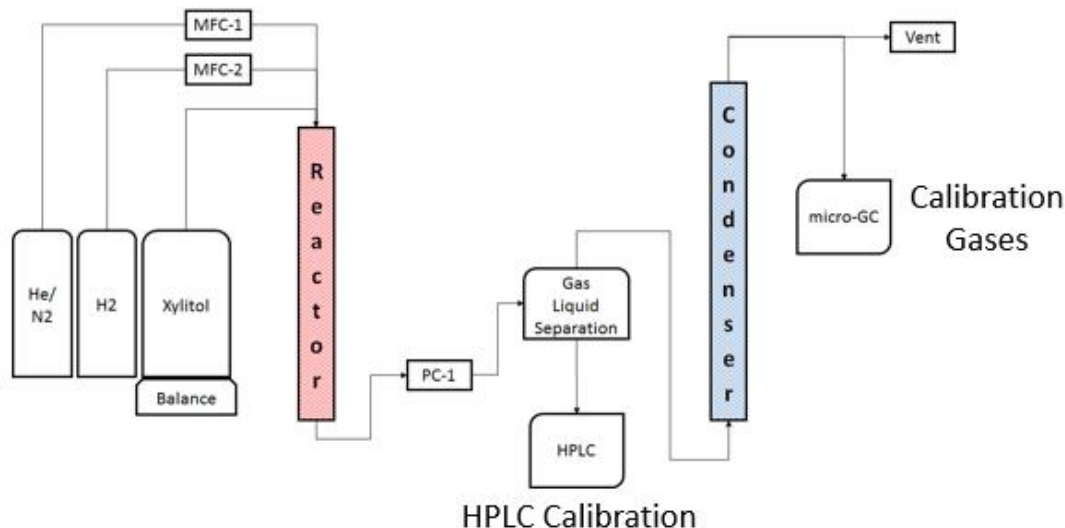


Figure 5 Experimental set-up for aqueous phase reforming.

The hydrogen line in Figure 5 is used during reduction of the catalyst while is done at 250°C with a constant flow of hydrogen for 2 hours. Heating to the desired temperature under hydrogen flow is done at a ramp 5°C by minute.

2.1.2 Micro gas chromatograph (micro-GC) calibration:

The micro-GC used in the experiment was Agilent 3000A. Calibration is done for 17 gases (Table 1). Twelve alkanes between C1 to C7, hydrogen, carbon dioxide, nitrogen, helium and carbon monoxide were calibrated. The calibration was made taking 10 samples of each gas.

Table 1 Gases calibrated in the micro GC.

Gases					
carbon dioxide	iso-butane	iso- pentane	n- hexane	helium	methane
ethylene	n-butane	n-pentane	cyclic hexane	hydrogen	carbon monoxide
propylene	neo- pentane	iso-hexane	n- heptane	nitrogen	hydrogen

2.1.3 High pressure liquid chromatograph calibration

The high pressure liquid chromatograph (HPLC) is a Hewlett Packard serie 1100. For HPLC analysis first it was necessary to identify different substrates present in the liquid samples. After the substrate identification the calibration was made for 28 compounds (Table 2). Every compound was calibrated with 3 different solutions having concentration 1wt%, 0.5wt% and 0.25wt%. For formic acid, a sample of 2wt% was added. In the case of ethylene glycol, glycerol, erythritol, xylitol, xylose and sorbitol a sample with 3wt% was added.

Table 2 Substrates calibrated by HPLC.

Substrates			
furfural	xylitol	glycerol	propane-1,2-diol
xylose	erythritol	formaldehyde	propane-1,3-diol
sorbitol	glycolaldehyde	formic acid	acetaldehyde
dulcitol	glycolic acid	acetic acid	methanol
arabitol	lactic acid	ethylene glycol	1-2 butane diol
ethanol	iso propanol	1,2 pentane diol	1 butanol
butyric acid	1 propanol	butyraldehyde	1,2 hexanodiol

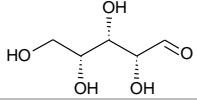
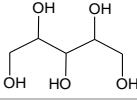
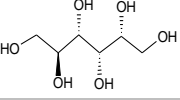
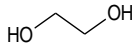
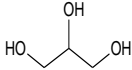
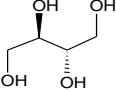
2.1.4 Experiments:

The substrate were tested in two kinds of experiments. The first one was with just 3wt% of a substrate while in the second in addition to this amount also contained 2wt% of formic acid. The liquid flow was 0.2 ml/min per gram of catalyst and the gas

flow was 72.8 ml/min per gram of catalyst. During the experiment three different temperatures were tested 175, 200 and 225°C. The pressure was fixed at 32 bar. The utilized substrates are shown in Table 3.

The experiments with formic acid in solution were done to observe the behavior of the real feed in the reactor and to detect interactions with the substrates. Because formic acid could be used for biomass hydrolysis.

Table 3 Substrates.

Xylose	Xylitol	Sorbitol
		
Ethylene Glycol	Glycerol	Erythritol
		

2.1.5 Calculations of conversion, selectivities and yields

The following equations were used to quantify the products of different experiments.

The conversion of the substrates was calculated as:

$$X (\%) = \frac{C_{in} - C_{out}}{C_{in}} * 100\%$$

When C_{in} is the inlet concentration and C_{out} is the outlet concentration.

The hydrogen selectivity was defined as:

$$H_2 \text{ selectivity } (\%) = \frac{\text{flow of hydrogen} * 2}{\text{total amount of hydrogen in the gas phase molecules}} * 100\%$$

Where the flow is defined in mol/min. The total amount of hydrogen in the gas phase molecules correspond to the sum of every identified molar flow by the number of hydrogen mols in the respective molecule.

Selectivity to carbon dioxide, carbon monoxide and the alkanes was calculated as:

$$\text{Product selectivity } (\%) = \frac{\text{carbon in the product}}{\text{total amount of carbon in the gas phase molecules}} * 100\%$$

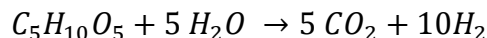
The amount of carbon was quantified in mol/min. The total amount of carbon in the gas phase molecules correspond to the sum of every identified molar flow by the number of carbon mols in the respective molecule.

The yield of different products was calculated as:

$$\text{Yield}_{\text{Product with C}} = \frac{\text{Product } \left[\frac{\text{mol}}{\text{min}} \right] * n^{\circ} \text{ of C in the product}}{\text{Initial concentration} * n^{\circ} \text{ of C in the substrate} * \text{inlet flow } \left[\frac{\text{ml}}{\text{min}} \right]}$$

$$\text{Yield}_{\text{Hydrogen}} = \frac{\text{Product } \left[\frac{\text{mol}}{\text{min}} \right]}{\text{Initial concentration} * n^{\circ} \text{ of expected hydrogen moles} * \text{inlet flow } \left[\frac{\text{ml}}{\text{min}} \right]}$$

The inlet flow corresponds to the amount of the liquid flow pumped inside the reactor. The number of expected hydrogen moles generated per mole of xylose is equal to 10 according to:



The yield calculations were used in the effect of catalyst composition experiments for observe the best catalyst composition for aqueous phase reforming of xylose with formic acid.

2.1.6 Results:

The experiments were analyzed by substrate effect, alkane behavior, liquid phase composition and liquid - gas carbon distribution. Using the 45 molecules identified

and calibrated with a high reliability by the good carbon identification expressed in the carbon balance analysis.

The effect of the catalyst composition was done just for the mixture xylose and formic acid to improve the APR performance in sugars.

Finally, all the data was used in the discussion to confirm the presence of some reaction pathways and also to suggest some reactions related to the products.

2.2 Substrate effect

Several experiments have been done with a catalyst containing 2.5 wt% platinum and 0.6 wt% palladium supported on mesoporous carbon. The substrates were ethylene glycol, glycerol, erythritol, xylitol, xylose and sorbitol.

During the tests the polyols substrates displayed similar behavior. These molecules exhibited a high selectivity to hydrogen and carbon dioxide. Presence of formic acid decreased selectivity to alkanes and carbon monoxide. Formic acid itself showed complete conversion at all temperatures.

Xylose displayed behavior different from polyols. Selectivity was high to carbon dioxide while for alkanes and hydrogen it was low and comparable. Formic acid increases the amount of alkanes without generating a substantial decrease in selectivity to carbon dioxide.

2.2.1 Ethylene Glycol

The experiments with ethylene glycol were performed at 200°C and 225°C. The results showed the conversion of ethylene glycol changing with the conditions (Figure 6). However selectivity displayed to be stable for all conditions (Figure 7).

The experiments with ethylene glycol exhibited an increase in the activity with temperature elevation. The conversion displays variability with the time on stream. The selectivities to hydrogen and carbon dioxide were near to 100% in both conditions. The selectivities of alkanes and carbon monoxide for this conditions were close to zero.

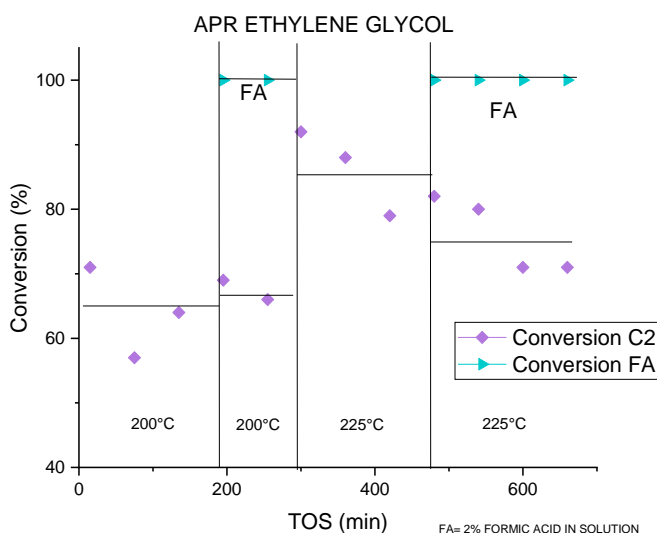


Figure 6 Conversion for ethylene glycol aqueous phase reforming.

The experiments with formic acid displayed a total conversion for formic acid in both conditions while the ethylene glycol conversion increased with temperature. Moreover the ethylene glycol activity exhibited to be different in comparison with the experiment in absence of formic acid. The selectivity did not change with the formic acid addition and was maintained in time being almost 100% for H₂ and CO₂.

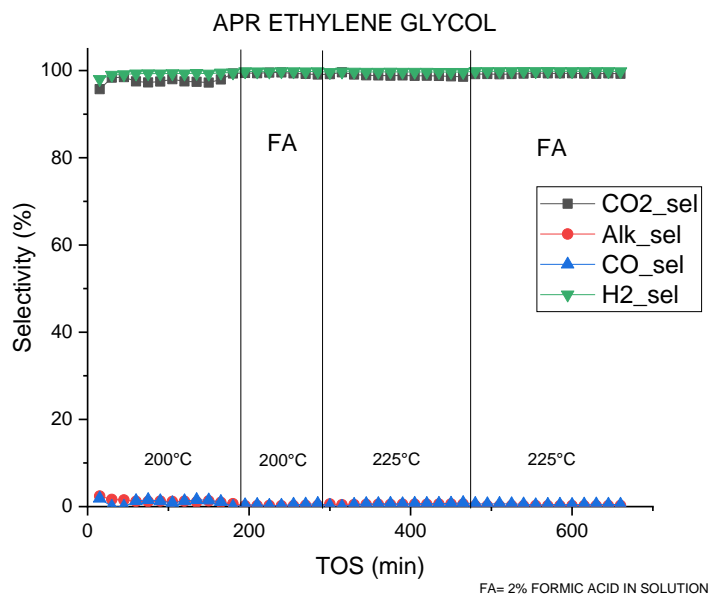


Figure 7 Selectivity graph of ethylene glycol APR.

2.2.2 Glycerol

Experiments with glycerol were performed at two temperatures 200°C and 225°C. The activity did not present important changes with the conditions (Figure 8). The selectivity displayed differences in each condition (Figure 9).

The glycerol experiment displayed a stable behavior where conversion increased with the temperature increase. The selectivity displayed changes with the conditions. The selectivities to hydrogen and alkanes did not change with the condition. Carbon dioxide showed a decrease with the temperature increase related to the carbon monoxide increase. Selectivities were rather stable in time.

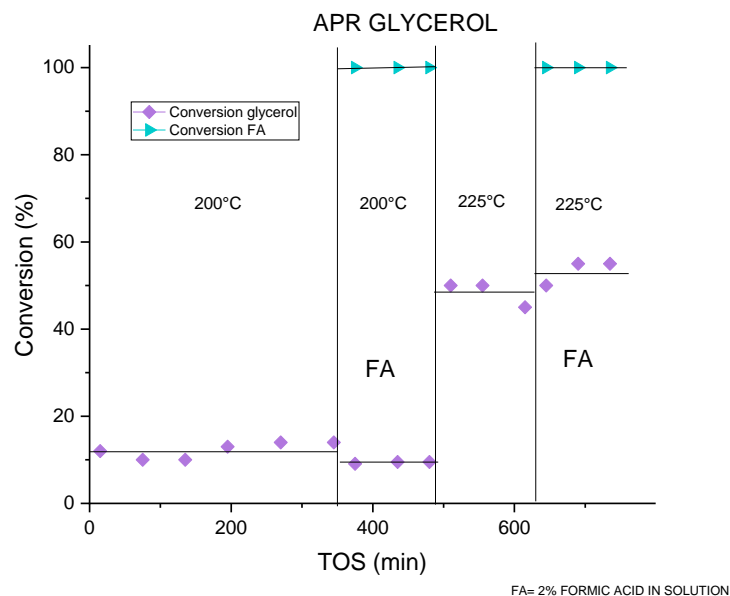


Figure 8 Conversion for glycerol aqueous phase reforming.

The experiments in presence of formic acid exhibited a similar activity for glycerol while the formic acid was converted completely. The selectivities displayed changes with the conditions. Formic acid causes a decrease in the alkane and carbon monoxide production making possible an elevation in the selectivities to hydrogen and carbon dioxide. The formic acid effect over the selectivity decrease with the temperature rise.

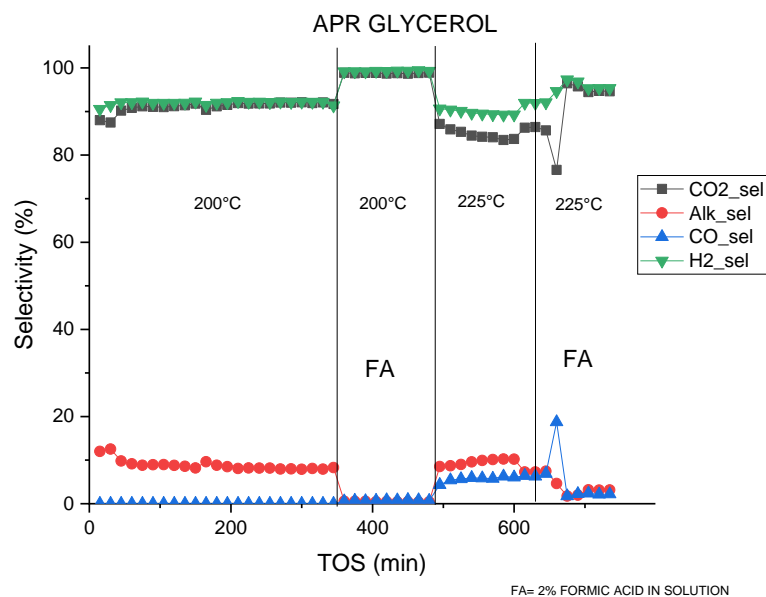


Figure 9 Selectivity graph of glycerol APR.

2.2.3 Erythritol

Experiments with erythritol were performed at two temperatures 200°C and 225°C. The conversion displayed changes with feed and temperature (Figure 10). Selectivity illustrates high hydrogen and carbon dioxide production (Figure 11).

The activity of erythritol experiments were improved by temperature rise. At low temperature conversions showed to be stable while at high more variability was observed. At both temperatures the selectivities were similar. Just at 225°C the selectivity to CO₂ decreased by an increase in the CO production.

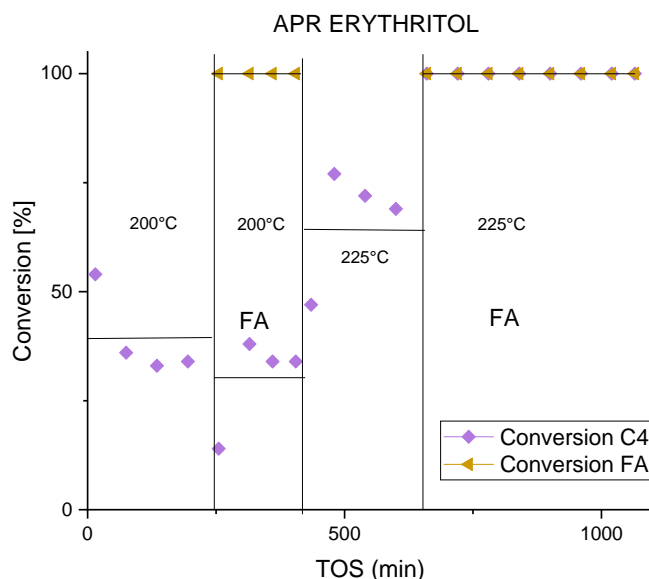


Figure 10 Conversion for erythritol aqueous phase reforming.

The experiment with formic acid displayed a similar conversion at low temperature and an increment in the activity with an increase in the temperature. Conversion of formic acid was complete in the whole temperature range. Formic acid had a positive effect on selectivity to hydrogen. The alkane selectivity increased with the temperature.

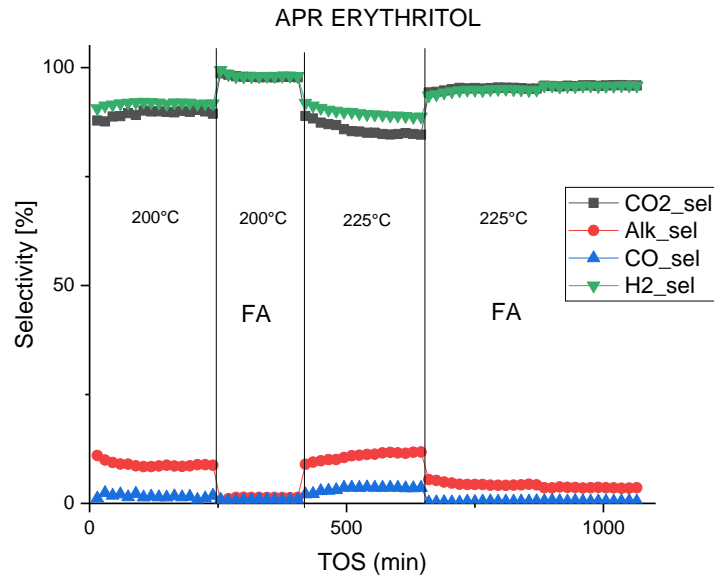


Figure 11 Selectivity graph of erythritol APR.

2.2.4 Xylitol

Experiments with xylitol were performed at two temperatures 200°C and 225°C. In the xylitol experiments conversion was high and stable (Figure 12). The temperature increase induced higher activity. The hydrogen and carbon dioxide selectivities were high (Figure 13). At 225°C the CO₂ selectivity decreased due to an increase of the selectivity to alkanes. Carbon monoxide was absent in all conditions.

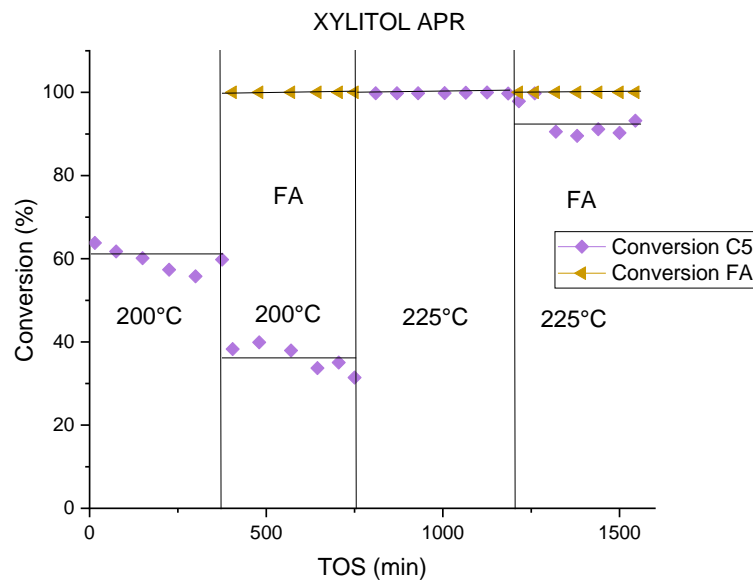


Figure 12 Conversion for xylitol aqueous phase reforming.

The formic acid experiments exhibited a decrease in the xylitol activity while the formic acid conversion was complete at both temperatures. The formic acid showed improved selectivity to hydrogen. However the alkane selectivity increased with an elevation in the temperature.

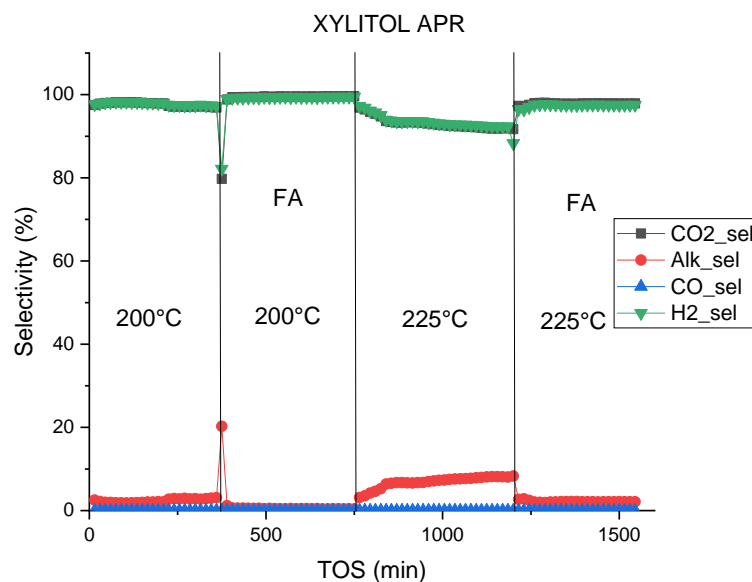


Figure 13 Selectivity graph of xylitol APR.

2.2.5 Xylose

Experiments with xylose were performed at three temperatures 175, 200 and 225°C. The xylose experiment at 225°C is not shown in Figure 14 and 15 because at that temperature xylose clogged the reactor. However, formic acid made possible the operation at higher temperature.

In the xylose experiments the conversion was stable and complete for both conditions (Figure 14). The selectivities to H₂ and CO₂ were the higher ones (Figure 15). While the selectivity to alkanes increased during the experiments. Temperature elevation displayed a negative in hydrogen selectivity but produced a decrease in the CO production.

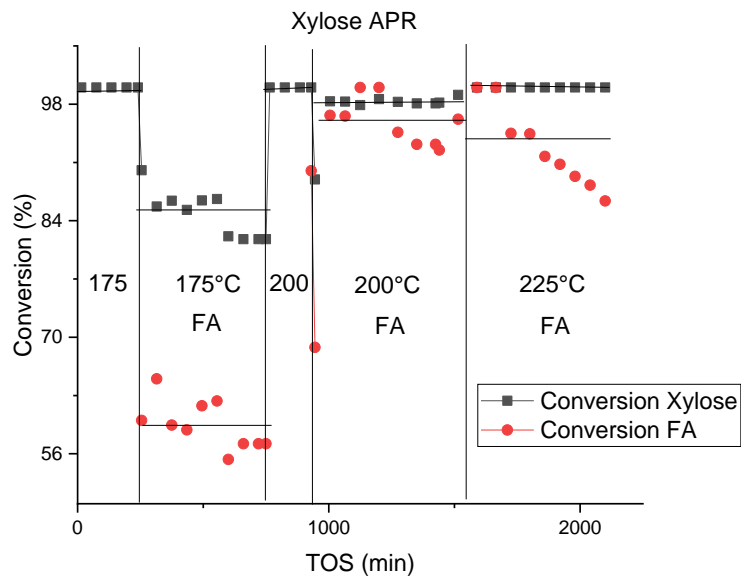


Figure 14 Conversion for xylose aqueous phase reforming.

In the experiments with formic acid it was possible to observe a different behavior. During the operation it could be noticed that the formic acid conversion was always lower than the xylose conversion. In addition formic acid produced a decrease in the xylose activity (Figure 14). Formic acid had an important role in increasing selectivity to alkanes and decreasing simultaneously selectivity to H₂. During these experiments the selectivity to carbon monoxide was higher too.

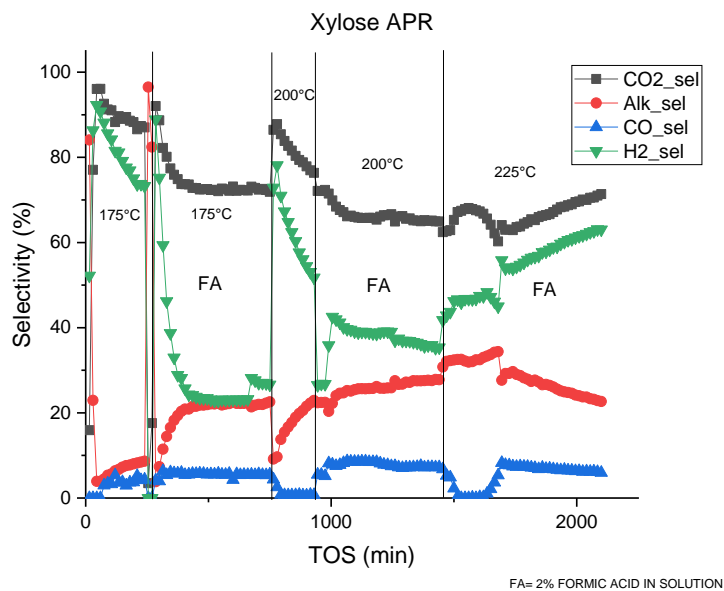


Figure 15 Selectivity graph of xylose APR.

2.2.6 Sorbitol

Experiments with sorbitol were performed at two temperatures 200°C and 225°C. The sorbitol experiment exhibited a high variability in the activity at low temperature while at high temperature the conversion was complete (Figure 16). The selectivities were similar at both temperatures characterized by a high production of hydrogen and carbon dioxide (Figure 17). The alkanes displayed c.a. 10% selectivity at both temperatures.

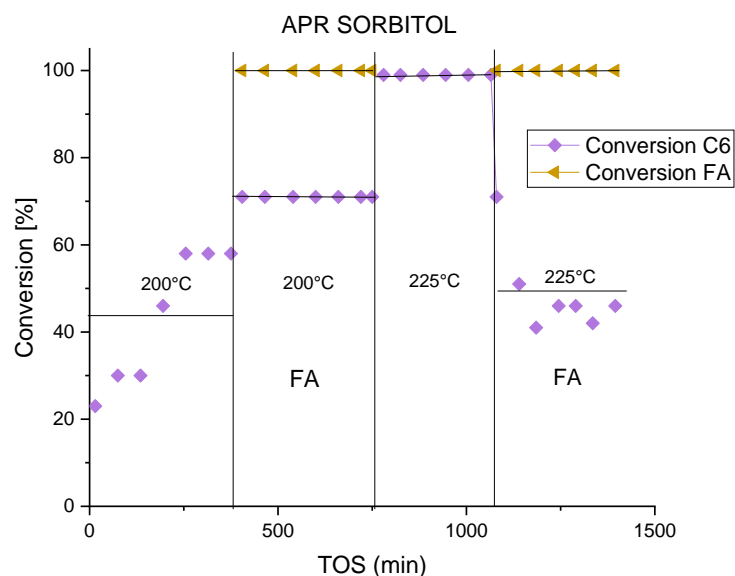


Figure 16 Conversion for sorbitol aqueous phase reforming.

The experiments with formic acid displayed an opposite behavior decreasing the conversion of sorbitol with temperature (Figure 16). The conversion of formic acid was complete at both temperatures. Formic acid produced an increase in the selectivities to hydrogen and carbon dioxide (Figure 17). Consequently the alkanes and carbon monoxide production were near to zero during this experiments.

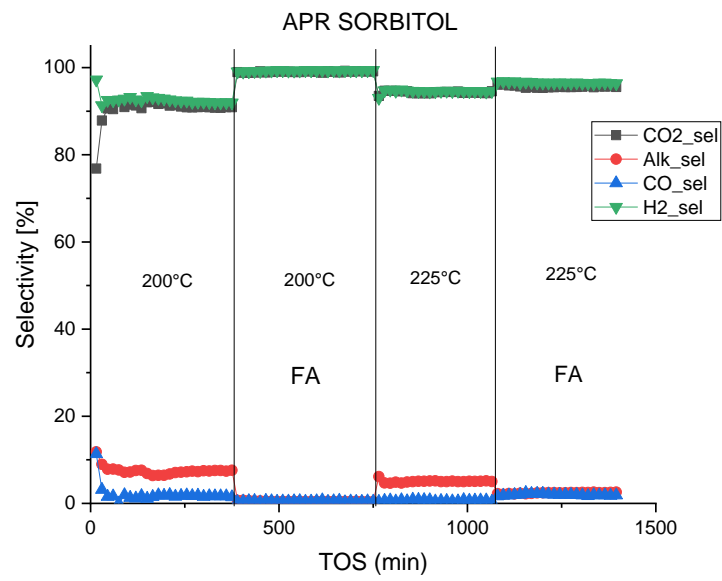


Figure 17 Selectivity graph of sorbitol APR.

2.3 Alkane behavior

In the aqueous phase reforming of polyols an important issue is the production of alkanes. Because these side products consume hydrogen making the process less attractive by the decrease in the H_2/CO_2 ratio. Hence during the experiments the flow of each alkane was quantified.

The results illustrated that the alkane distribution was related to the substrate. Polyols other than xylitol had a similar behavior with a rather constant distribution at all temperatures and a decrease in selectivity with addition of formic acid. On the contrary xylose displayed a different behavior with changes in the distribution with temperature and addition of formic acid.

Selectivity to alkanes in the APR of polyols was low with a maximum selectivity close to 7% for methane in the glycerol aqueous phase reforming while for xylose the maximum value was 20% for pentane production at 225°C in the presence of formic acid.

2.3.1 Ethylene glycol

The ethylene glycol aqueous phase reforming had a high selectivity to hydrogen and carbon dioxide. Thus selectivity to alkanes was low (Figure 18). A higher selectivity was displayed by butane at 200°C not exceeding 0.4% average. After butane the most important alkane was methane with 0.2% of selectivity.

During the experiments with formic acid selectivity to each alkane was lower than 0.1% with methane being the most important alkane in these experiments.

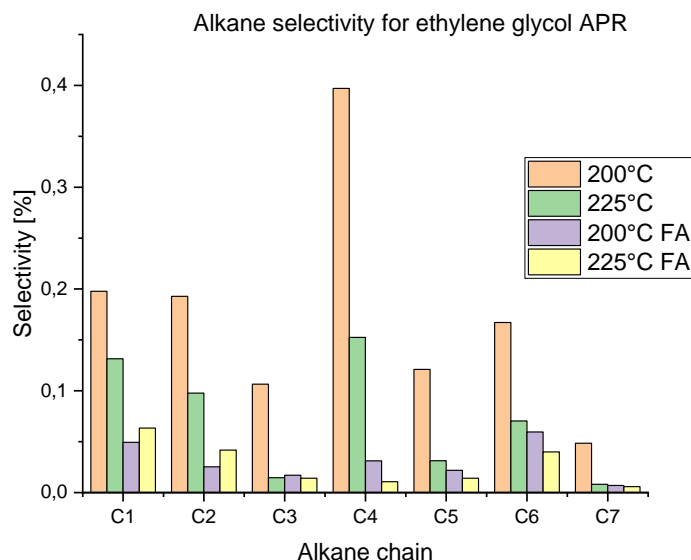


Figure 18 Alkane selectivity for ethylene glycol APR.

2.3.2 Glycerol:

The experiment with glycerol shows (Figure 19) rather high selectivity to methane i.e. 8%. Other alkanes exhibited a low selectivity. Presence of formic acid diminished selectivity to alkanes with the magnitude dependent on temperature.

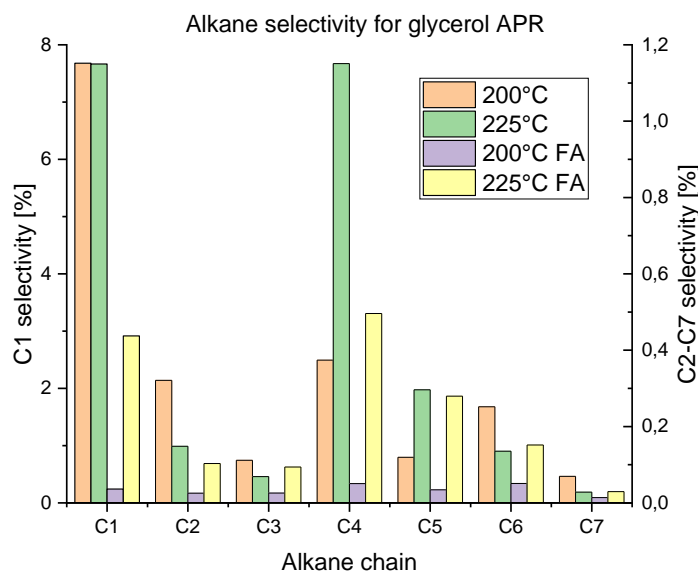


Figure 19 Alkane selectivity for glycerol APR.

2.3.3 Erythritol:

Erythritol APR (Figure 20) shows a high selectivity to ethane followed by methane. Distribution of alkanes did not change with temperature. Introduction of formic acid resulted in a decrease in the alkane production without changes in their distribution.

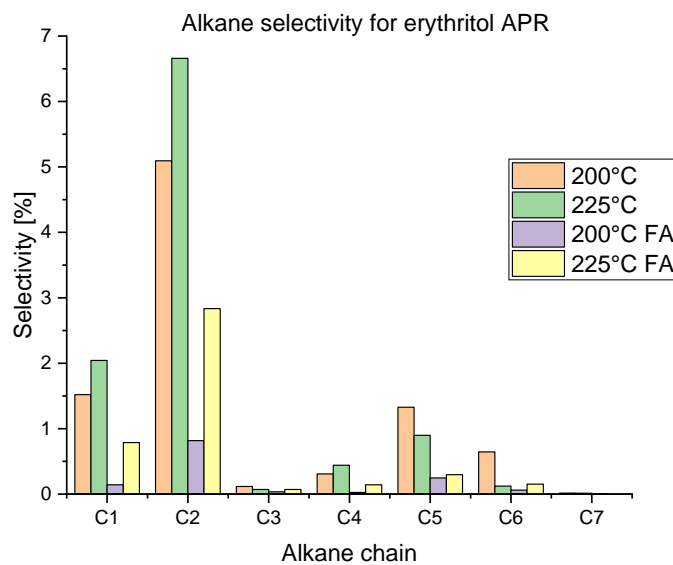


Figure 20 Alkane selectivity for erythritol APR.

2.3.4 Xylitol

Figure 21 displays a low selectivity to alkanes with similar values to methane, ethane and propane. The maximum selectivity was around 3% for ethane and methane was exhibiting a similar selectivity. When formic acid was added, overall selectivity to alkanes was lower, however, without changes in the alkane distribution. Influence of formic acid was less prominent upon temperature elevation.

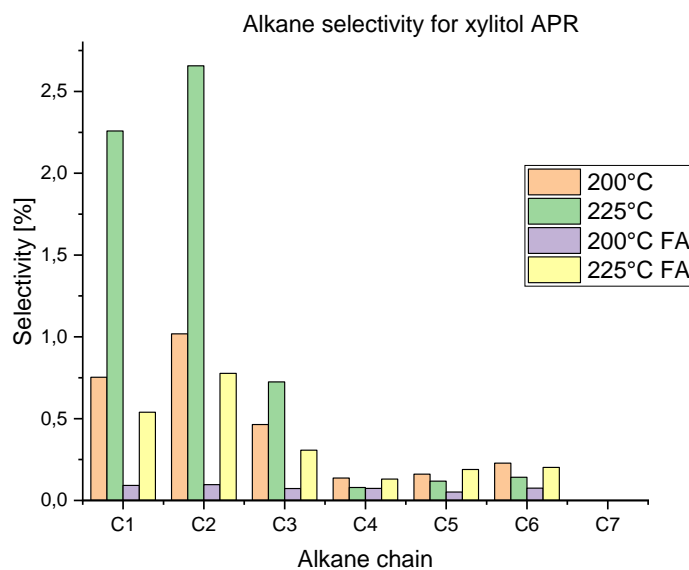


Figure 21 Alkane selectivity for xylitol APR.

2.3.5 Xylose

Xylose APR presents a high selectivity to alkanes with a maximum of 18% at 225°C for pentane (Figure 22). There was a dependence of alkane distribution on temperature. Formic acid increased selectivity to alkanes and had an influence on the alkane distribution.

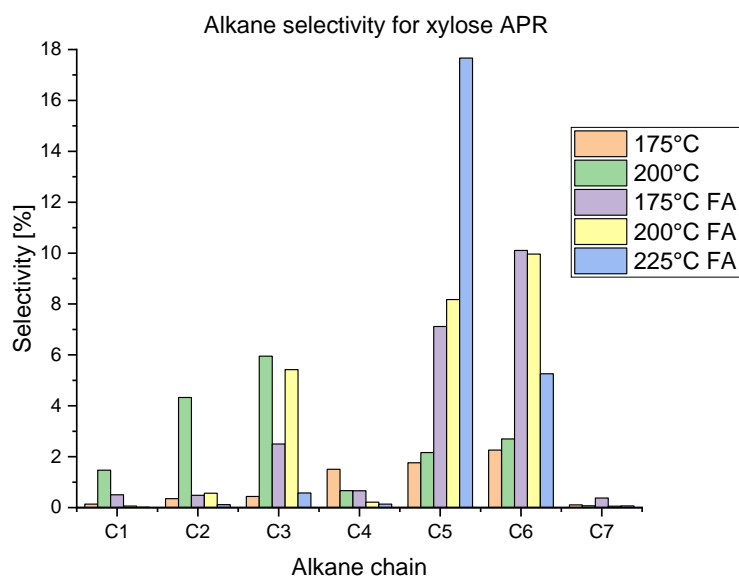


Figure 22 Alkane selectivity for xylose APR.

2.3.6 Sorbitol

Selectivity in sorbitol APR (Figure 23) to alkanes was low with a maximum 2.4%. Methane and ethane were the main products among alkanes. Similar to xylitol APR presence of formic acid did not result in changes in the alkane distribution but led to a decrease in the alkane selectivity. Less alkanes were formed when the temperature was increased. The effect of formic acid on selectivity to alkanes was temperature dependent.

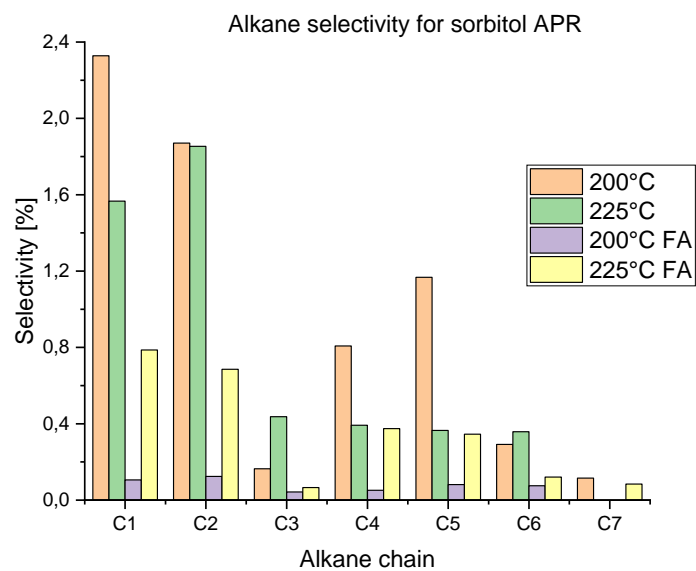


Figure 23 Alkane selectivity for sorbitol APR.

2.4 Liquid phase composition

During the aqueous phase reforming product analysis of the liquid phase is one of the largest challenges. As reported by Kirilin et al. in APR of sorbitol over 260 compounds could be identified [25]. Therefore it is necessary to have a clear determination of the major products to close the mass balance.

During this work, it was possible to find 28 reaction products of the liquid phase. The main identification was for ethylene glycol and glycerol with a 100% HPLC area recognition. The liquid identification for erythritol and sorbitol APR was possible with a 100%. For xylitol determination of compounds was equal to 80% while for xylose it was 70%. In the following figures for the liquid were reported just for the compounds identified in every sample.

Determination of C2 and C3 polyols among reaction intermediates of larger molecules shows that majority of polyols could have similar reaction paths. Some specific paths cannot be quantified with smaller molecules, for example, C5 furan chemistry is very rich and different from compounds with a lower or a higher carbon number.

2.4.1 Ethylene glycol:

Distribution of the liquid phase products in ethylene glycol APR given in Figure 24 shows 5 intermediates with low concentrations. Methanol exhibited the highest concentration which was increasing with temperature. In addition presence of glycerol in the liquid phase suggests condensation reactions.

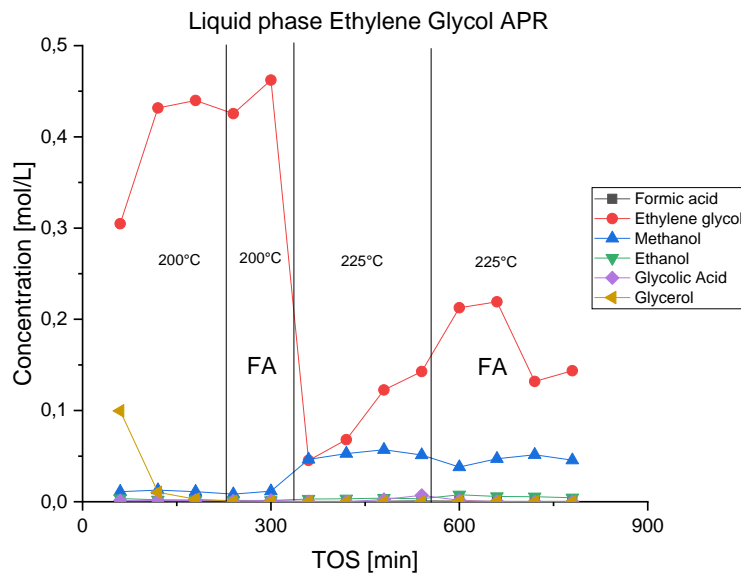


Figure 24 Liquid distribution in ethylene glycol APR.

2.4.2 Glycerol:

The liquid phase in APR of glycerol (Figure 25) is characterized by low concentrations of intermediates. At 200°C the most abundant product was ethanol while at 225°C propane diols were more prominent. Distribution of the liquid phase products was stable upon different conditions. Moreover APR of the mixture between formic acid and glycerol resulted in a decrease in the intermediates concentration.

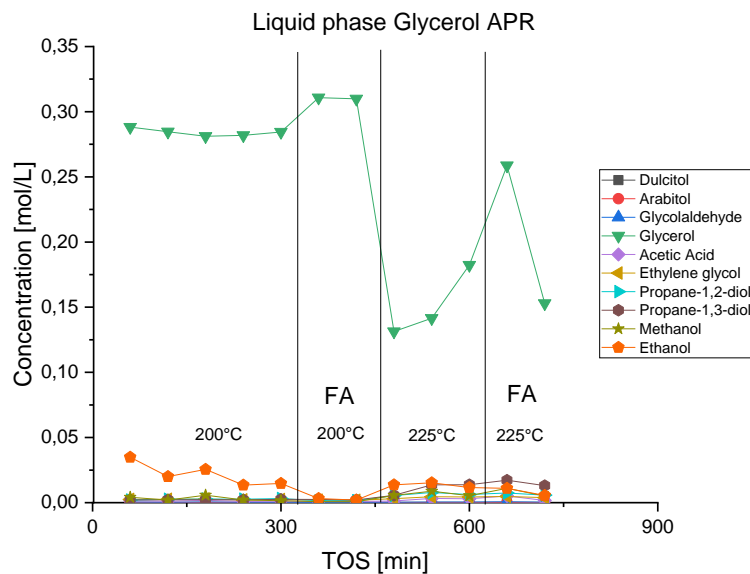


Figure 25 Liquid distribution in glycerol APR.

2.4.3 Erythritol:

The liquid phase of erythritol APR (Figure 26) is characterized by a substantial amount of methanol with a maximum 0.15M at 225°C in the presence of formic acid. Propane diol exhibited the second largest concentration. The distribution of the liquid product was the same under different conditions.

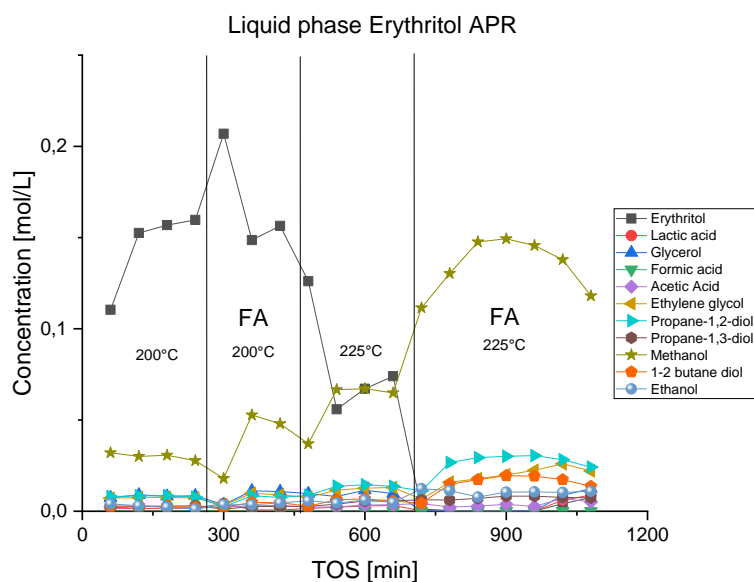


Figure 26 Liquid distribution in erythritol APR.

2.4.4 Xylitol:

In the case of xylitol APR the liquid phase (Figure 27) contained compounds in low concentrations. The most abundant was methanol with the concentration of 0.05 M at 225°C. There was no influence of reaction conditions on the product distribution.

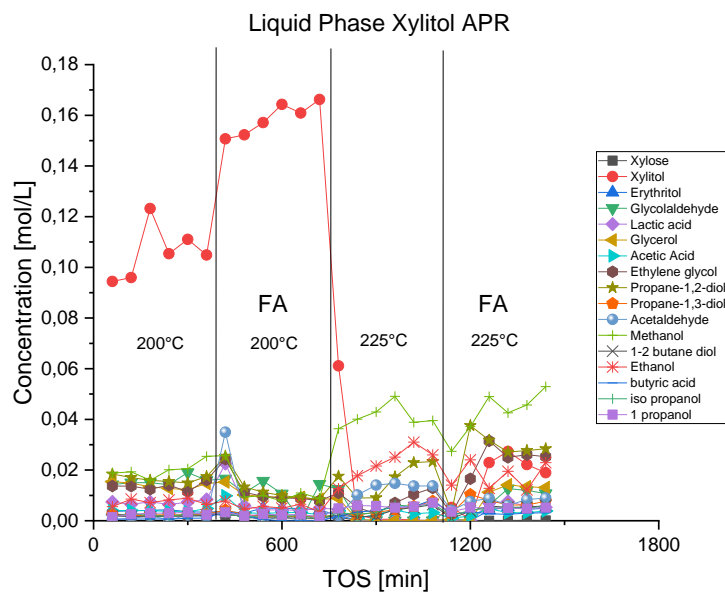


Figure 27 Liquid distribution in xylitol APR.

2.4.5 Xylose:

A high amount of intermediates was observed in the liquid phase for xylose APR (Figure 28) with the maximum concentration reaching 0.04M. There was a clear influence of reaction conditions on the product distribution. For example at 175°C formic acid and xylose did not react completely.

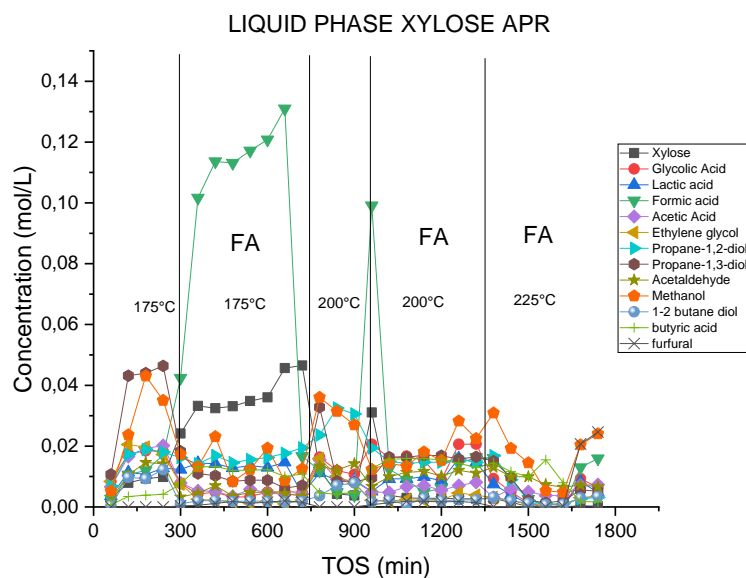


Figure 28 Liquid phase distribution of products in xylose APR.

2.4.6 Sorbitol:

Distribution of the liquid phase products in sorbitol (Figure 29) was constant with time on stream. Methanol was the most important intermediate followed by propane diol and ethylene glycol. The higher concentration of methanol was 0.05 M.

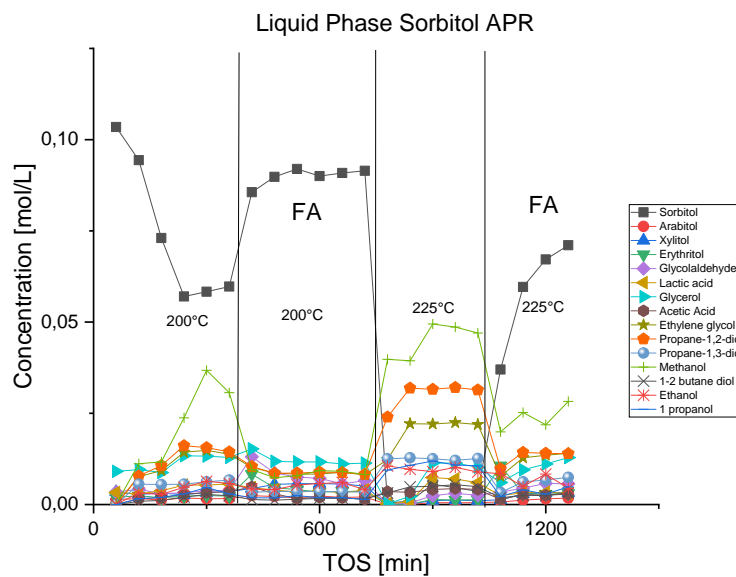


Figure 29 Distribution of the liquid phase products in the APR of sorbitol.

2.5 Liquid - Gas carbon distribution:

From analysis of the gas and liquid phases it was possible to normalize the presence of each carbon chain in the products and make an analysis of the changes in the distribution depending on the conditions. The carbon distribution for polyols as ethylene glycol, glycerol, erythritol and sorbitol exhibited similarities between the compounds while xylitol and xylose displayed a complex behavior with different distribution upon varying conditions.

This analysis exhibited differences between the liquid and the gas phase. Moreover it is not possible to observe a clear correlation between the liquid products and the gas products distribution. Therefore it will be a helpful tool to analyze the presence of some reaction in the discussion.

2.5.1 Ethylene glycol:

The gas phase of ethylene glycol (Figure 30 a) displayed small differences due to changes in the conditions. Total selectivity to hydrocarbon was ca. 2% making quantification of alkanes difficult.

The liquid phase showed (Figure 30 b) a clear distribution with C2 compounds being the most important, followed by C1 substrates. Amounts of C3 compounds were low. The liquid phase exhibited a similar behavior at different conditions.

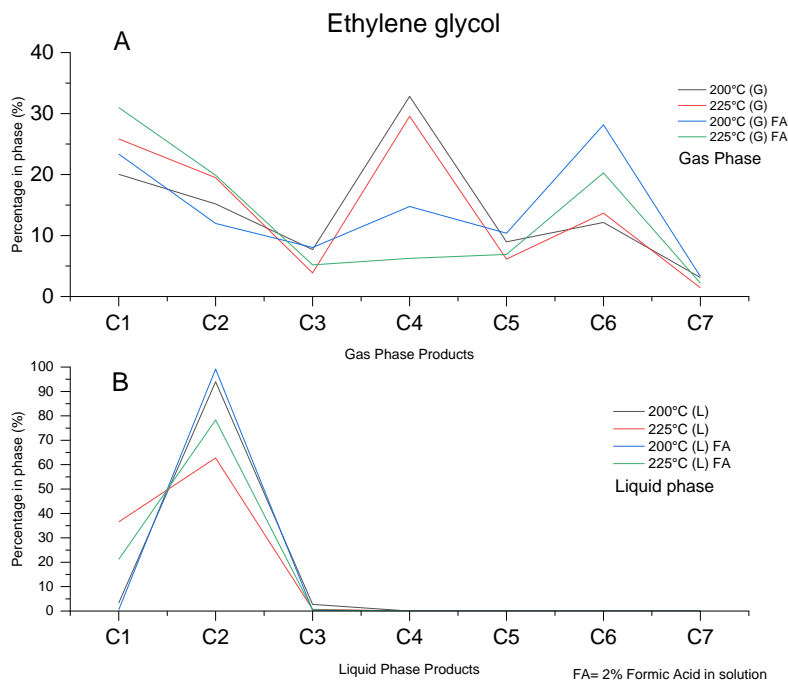


Figure 30 Distribution of (a) gas phase and (b) liquid phase products in ethylene glycol APR.

2.5.2 Glycerol:

The gas phase (Figure 31 a) in glycerol APR contained mainly methane and other alkanes in low concentrations. The second largest concentration after methane was exhibited by C4 compounds with a maximum of 12%. This can be related to aldol condensations.

The liquid phase (Figure 31 b) displayed a stable behavior with the C3 products being the most abundant with small amounts of C2 and C1 products. Moreover the largest carbon chains (C4+) were not detected.

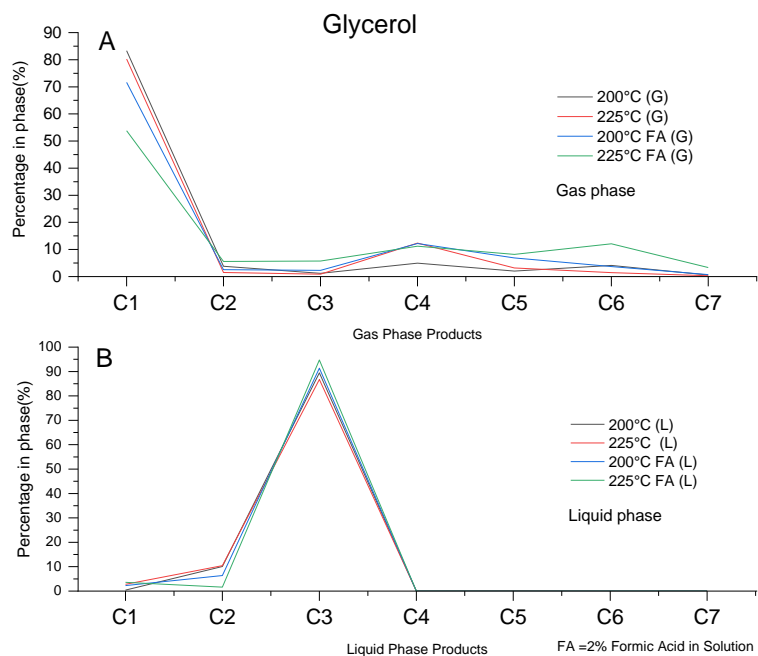


Figure 31 Distribution of (a) gas phase and (b) liquid phase products in glycerol APR.

2.5.3 Erythritol:

In erythritol APR the distribution in the gas phase shows small changes depending on conditions. Ethane was the most selective molecule followed by methane (Figure 32 a). In addition alkanes with the longer chain were present in low amounts (C5+), which can be due to polyols condensations.

The liquid phase had mainly C4 intermediates followed by C2 and C1 compounds in similar amounts (Figure 32 b). However, the amount of C4 decreased with elevation of temperature. The quantities of C2 and C1 became more prominent.

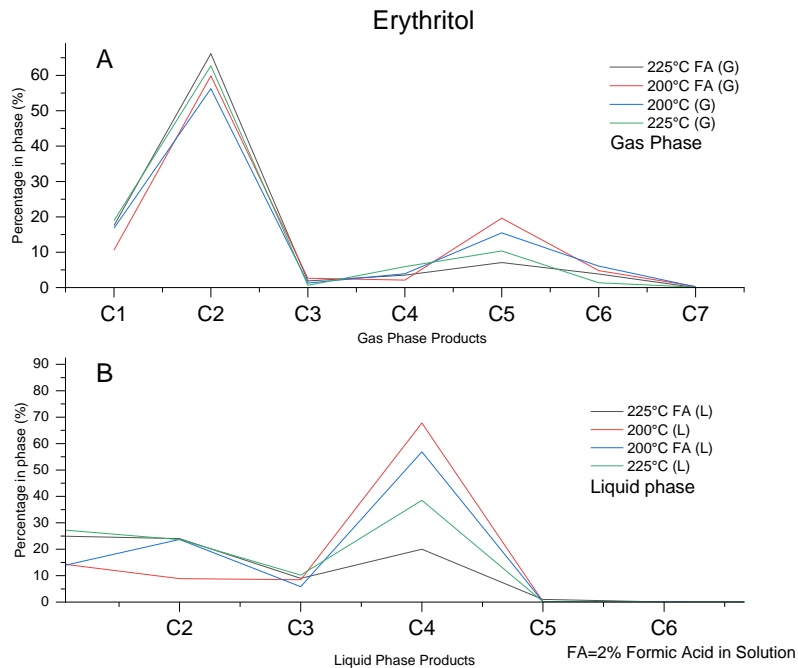


Figure 32 Distribution of (a) gas phase and (b) liquid phase products in erythritol APR.

2.5.4 Xylitol:

Distribution of gas phase product in xylitol APR (Figure 33 a) was related to the conditions. In the experiments just with xylitol the gas phase was contained mainly C2 products and methane. The experiment with formic acid and xylitol exhibited a different behavior with C4 and C6 chains being more important. However, the alkane production in these experiment was low with a selectivity near to zero.

The liquid phase (Figure 33 b) displayed a distribution composed mainly by products from C3 to C1. C4 products were present in low amount. Nevertheless the experiment with formic acid showed an important amount of C5 products.

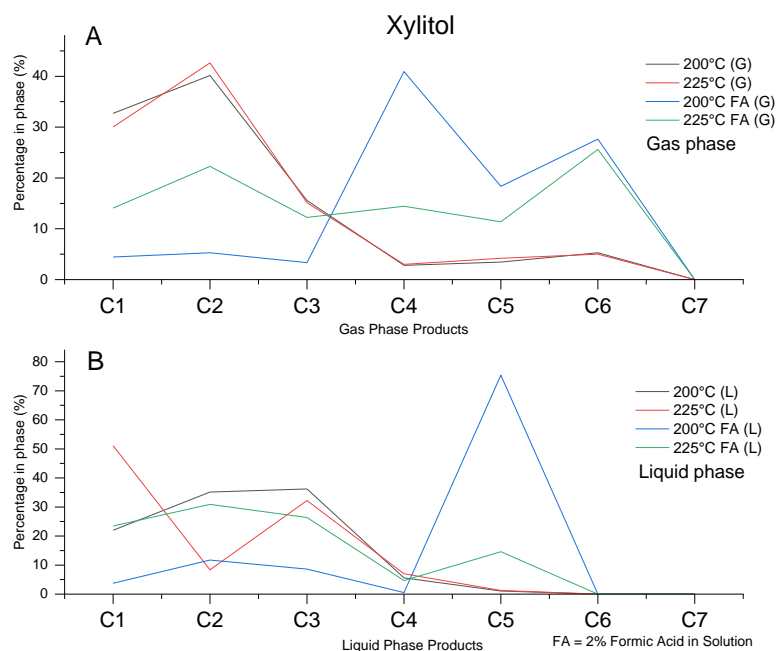


Figure 33 Distribution of (a) gas phase and (b) liquid phase products in xylitol APR.

2.5.5 Xylose:

Xylose APR gas products distribution (figure 34 a) exhibited an important amount of C5 and C6 chains. The C3 products were in low quantities. Moreover that distribution was maintained during different experiments with minor changes.

The liquid phase products were mainly from the C3 to C1 carbon chains (Figure 34 b). Nevertheless at low temperature without formic acid the C5 product was the most abundant in the phase. C4 content was low in most of the experiments.

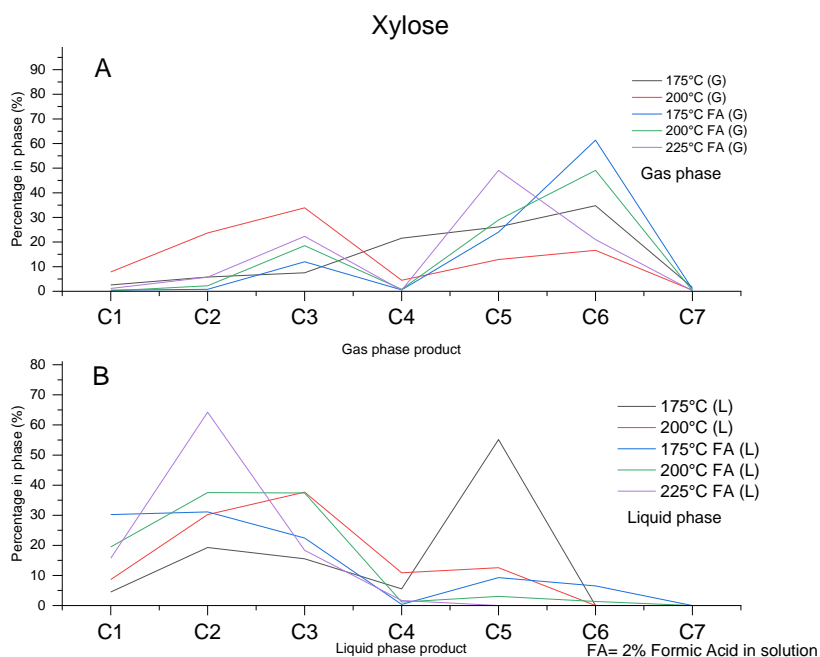


Figure 34 Distribution of (a) gas phase and (b) liquid phase products in xylose APR.

2.5.6 Sorbitol:

Sorbitol APR gas products displayed a rather stable behavior (Figure 35 a). The products were mostly C2 and C1. The longest chains (C3+) were present in similar amounts, with C4 and C5 being slightly higher.

The liquid phase (Figure 35 b) exhibited minor changes in the distribution in different experiments. The C6 products displayed the highest concentration. Moreover C3 to C1 products were in important amounts. C4 and C5 had similar quantities of ca. 5%.

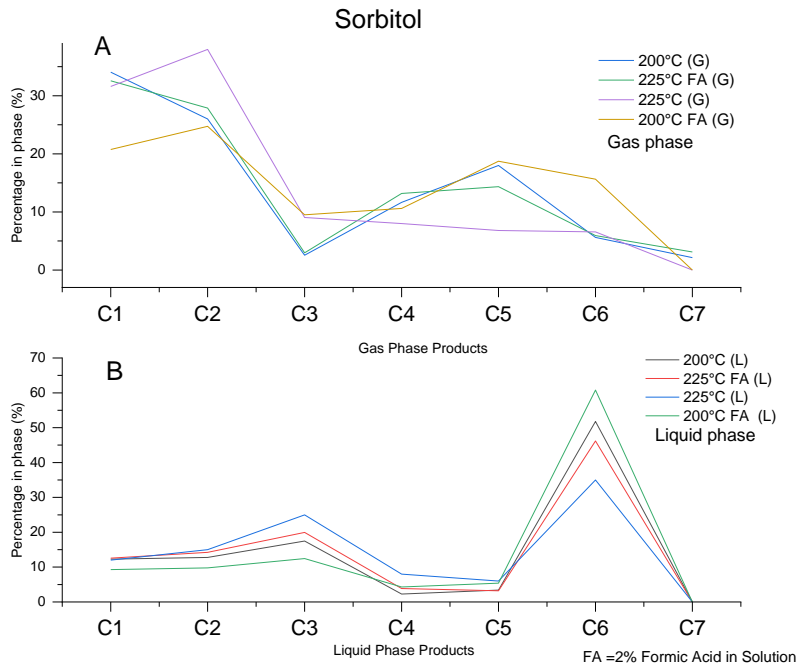


Figure 35 Distribution of (a) gas phase and (b) liquid phase products in sorbitol APR.

2.6 Carbon balance:

The carbon balance is a useful tool for the mass balance analysis. The carbon content was quantified in the liquid and the gas phases. Additionally it is possible to perform analysis of the best conditions to operate the system. Similarly it is easy to define the amount of carbon unknown in the products.

In xylose APR the lowest level of product identification was obtained (80%) followed by xylitol APR with 90% of carbon identification. Evaluation of the carbon balance was done by quantification of calibrated 45 molecules calibrated (28 in the liquid phase and 17 in the gas phase). More gas phase products were formed upon formic acid and temperature elevation.

Similar behavior between different substrates suggests similar reaction paths. It is important to note that unknown compounds in xylitol and xylose APR were different furans. Those molecules could not be properly identified during calibrations.

2.6.1 Ethylene glycol:

The carbon balance in ethylene glycol APR was complete at all conditions (Figure 36). The values above theoretical ones can be explained by experimental errors. The carbon balance showed that at 225°C most of carbon went to the gas phase. Formic acid presence did not result in changes in the carbon balance behavior.

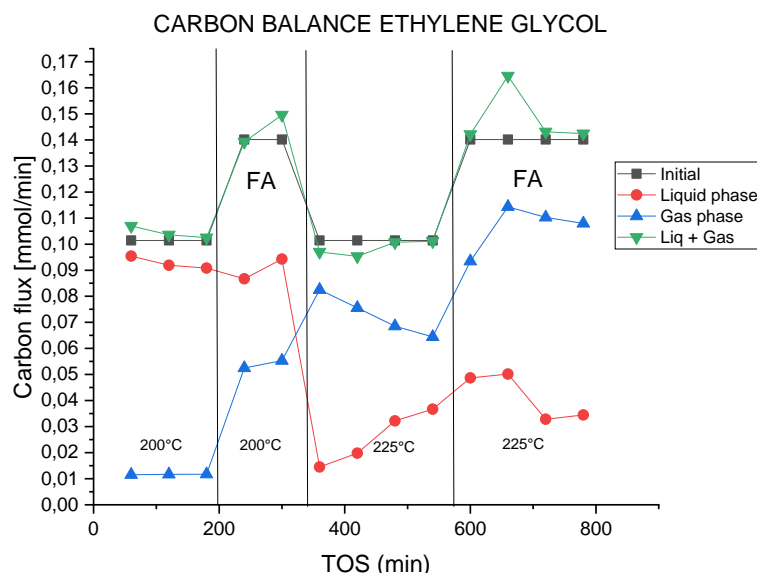


Figure 36 Carbon balance in ethylene glycol APR.

2.6.2 Glycerol:

The carbon balance for glycerol was complete (Figure 37). Most of carbon remained in the liquid phase at all conditions. Introduction of formic acid increased the amount of gas phase products at both temperatures.

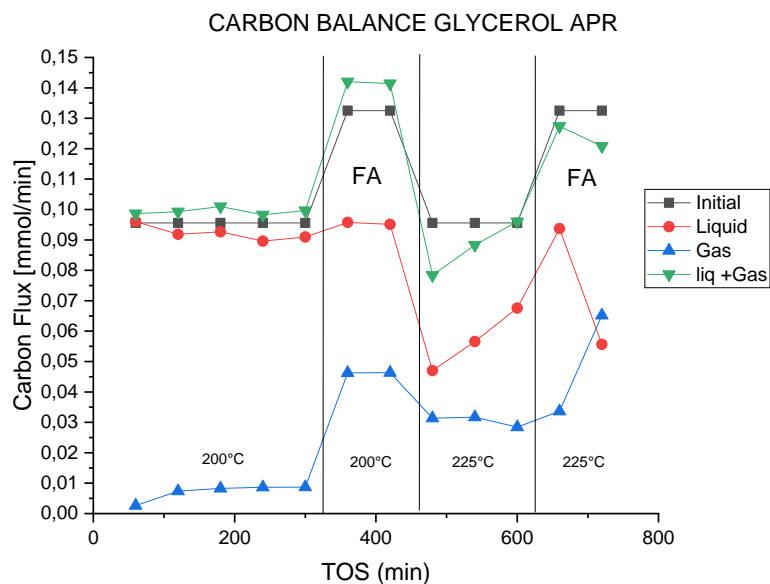


Figure 37 Carbon balance in glycerol APR.

2.6.3 Erythritol:

Erythritol APR displayed a complete carbon balance (Figure 38). At 225°C with formic acid it was possible to observe the experimental error and an increase in the gas phase products. In that sense operation at 225°C in the presence of formic acid was the optimal among the tested conditions because most of carbon went to the gas phase.

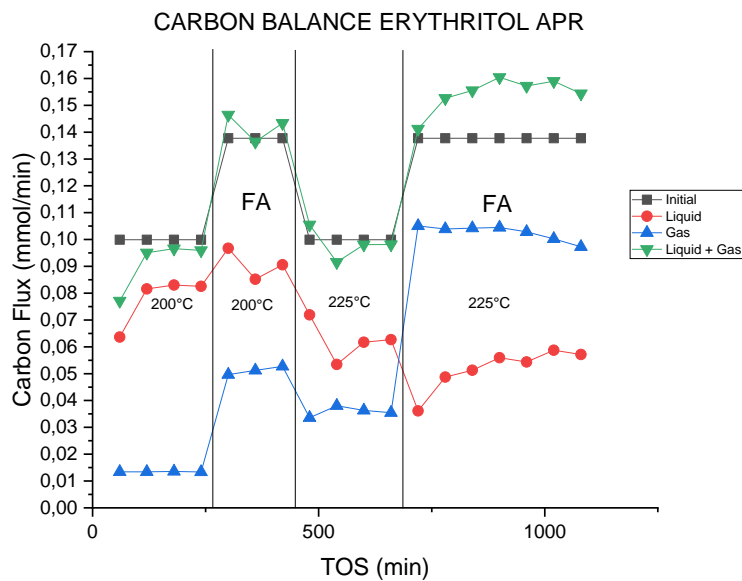


Figure 38 Carbon balance in erythritol APR.

2.6.4 Xylitol:

In xylitol APR it was possible to determine 90% of carbon containing compounds (Figure 39). The remaining 10% of unknown compounds can be attributed to derivatives of furans. Formic acid addition to xylitol gave incremental changes in the gas production.

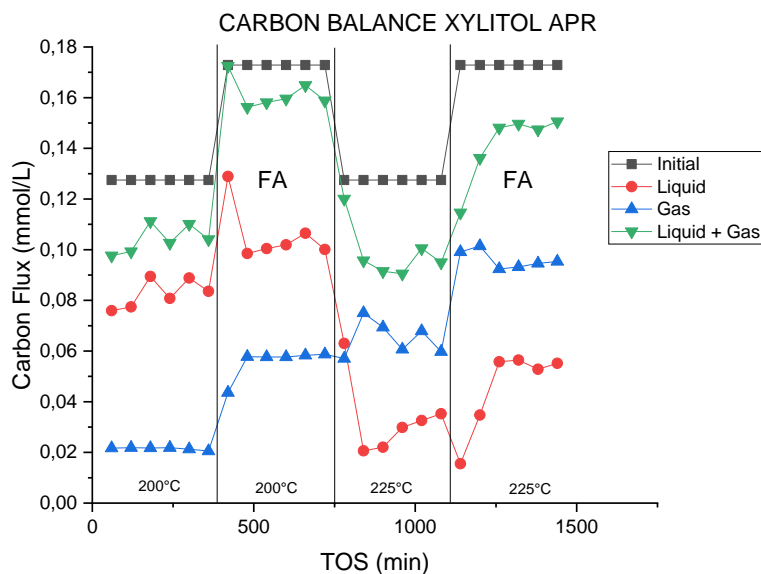


Figure 39 Carbon balance in xylitol APR.

2.6.5 Xylose:

In xylose APR 80% of carbon was identified (Figure 40). Above 200°C and in the presence of formic acid most of carbon was in the gas phase, while without formic acid the amount of gas products was low. The unknown carbon can be ascribed to furans.

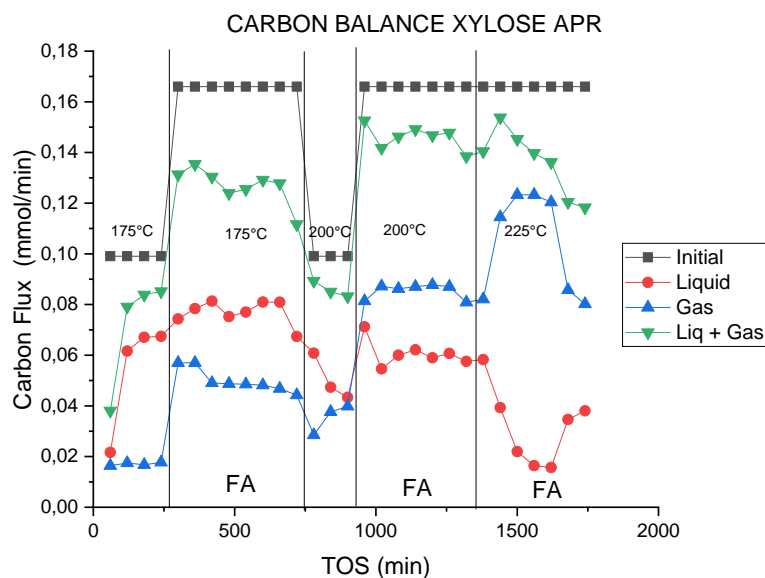


Figure 40 Carbon balance in xylose APR.

2.6.6 Sorbitol:

The carbon balance in APR of sorbitol was complete (Figure 41). Formation of gas phase products was important at 225°C in the presence and absence of formic acid.

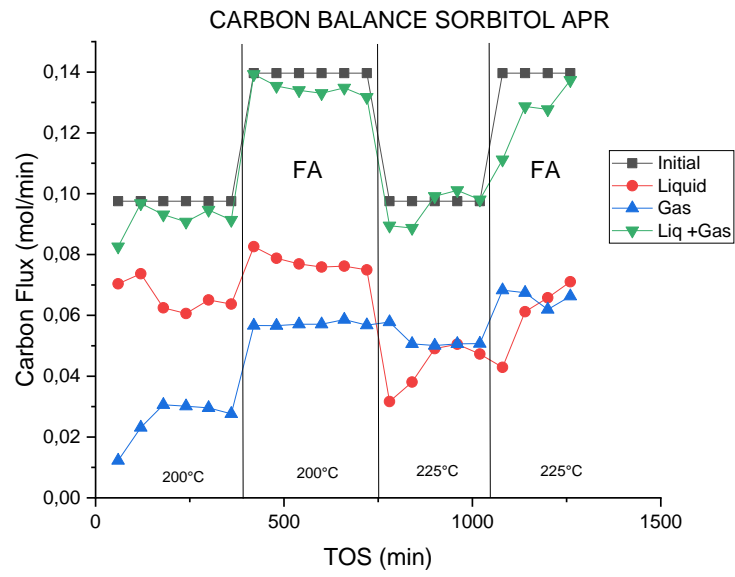


Figure 41 Carbon balance in sorbitol APR.

2.7 Effect of catalyst composition

The influence of the ratio between Pt and Pd was tested in APR of xylose with formic acid as this was relevant to a potential industrial application. The weight composition is given in Table 4.

Table 4 Catalyst tested.

Catalyst N°	Pt, wt%	Pd, wt%
1	2.50	1.25
2	0.60	2.50
3	2.50	0.60

Figure 42 exhibits all experiments together for an easy understanding of differences between the loadings. The experiments were done in the same conditions for every catalyst at a constant pressure of 32 bars. The gas phase was composed of nitrogen with a flow equal to 72.8 ml/min per gram of catalyst. The liquid phase was a mixture of 3 wt % xylose and 2 wt % formic acid pumped at a flow rate equal to 0.1 ml/min.

At 175°C every catalyst gave a similar carbon dioxide yield and ca. 10% of hydrogen yield. The alkane yield exhibited a similar behavior in the catalyst 1 and 2 while in the catalyst number 3 the yield was higher. For carbon monoxide it was lower for catalyst 1 being close to 0% while catalysts 2 and 3 displayed production of CO.

In experiments at 200°C the catalyst 1 shows higher selectivity to carbon dioxide while catalysts 2 and 3 exhibited small differences. The yield of alkanes was higher than for hydrogen in every experiment. Moreover, the yield of hydrogen was higher for catalyst 1 while the alkane selectivity was higher for catalyst 3. The carbon monoxide production was similar most of the time on stream, however the catalyst 1 showed an important decrease in the yield of this component.

The last experiments were done at 225°C. The deactivation at this temperature played an important role changing the yield of the products. Nevertheless the catalyst 1 presented the best behavior with a yield similar for hydrogen and alkanes and absence of carbon monoxide. The catalysts 2 and 3 revealed similar behaviors in production and deactivation. The carbon dioxide yield displayed an increment in time followed by an important deactivation. The catalyst 3 was the most selective to carbon dioxide.

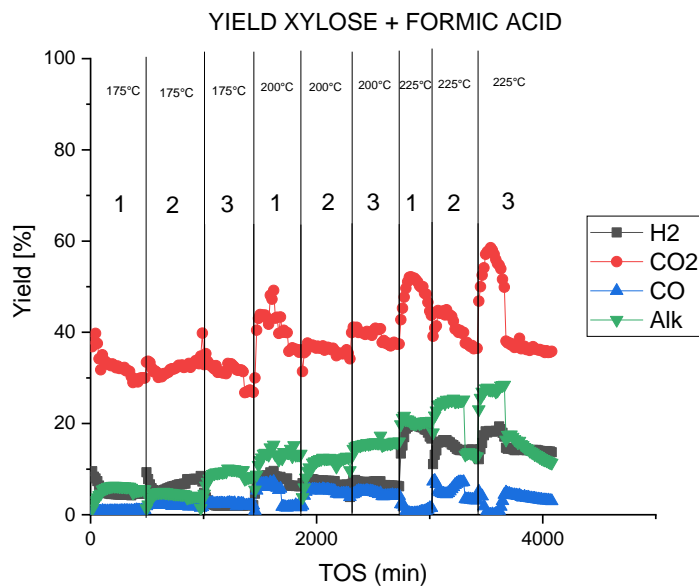


Figure 42 Yield of products in xylose with formic acid APR over different catalysts.

Figure 43 shows important changes with temperature in the alkane yield. At 175 °C the main product for each catalyst was C6 carbon chains with a higher selectivity in catalyst 3. Low amounts of C5 compounds were found.

At 200°C the C6 chains are the main products. Nevertheless the concentration of C5 compounds was increasing in each experiment. C3 products were observed in different amounts but never exceeding 4%. Catalyst 2 had the lowest production of alkanes at this temperature.

Experiments at 225°C exhibited significant changes during the time on stream. An increase of C5 products was observed until ca. 16% when they started to decrease fast for catalysts 2 and 3. The C3 compounds were changing during the entire experiment decreasing production over each catalyst. The catalyst 1 shows the lowest alkane yield, however, time of the experiment tested was lower for this catalyst consequently the deactivation effect was not entirely observed.

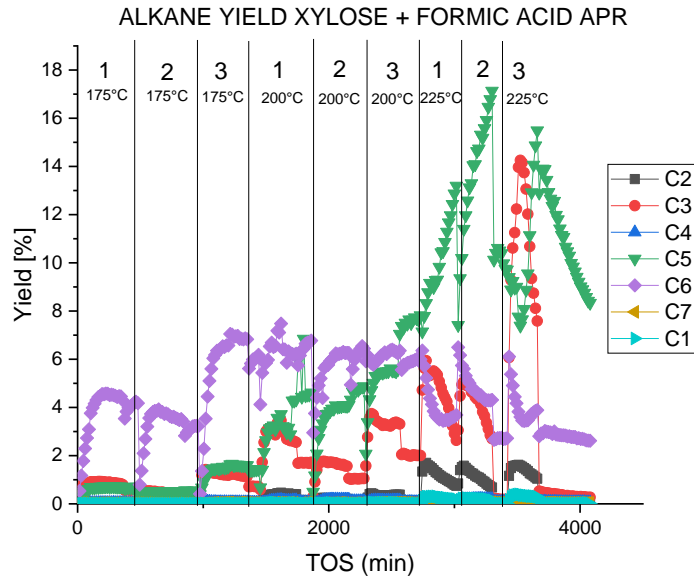


Figure 43 Yield of alkanes in APR of xylose with formic acid over different catalysts.

For this reason, the aqueous phase reforming of xylose in presence of formic acid shows to be affected by the catalyst composition. Catalyst 1 displayed the best performance for hydrogen production. Moreover, the absence of carbon monoxide could be an indicator of efficient WGS. Nevertheless longer experiments should be done in order to observe the steady state and complete deactivation.

2.8 Discussion

The activity was related to the substrate tested. The C5 (Xylose and Xylitol) compounds tested demonstrated different conversions. The sugar had almost complete conversion at all conditions while the polyol showed an activity temperature dependent. These observations suggest a dependence between the molecular nature and the APR performance.

The results show a clear dependence on the compound structure. The substrates with the same chain length but different terminal groups displayed different behavior. The substrates with an alcohol terminal group (xylitol) exhibited nearly no alkanes and carbon monoxide whereas the compounds which ended with a carbonyl group (xylose) were more selective to alkanes.

Higher acidity in the inlet flow resulted in an increase of selectivity to hydrogen and carbon dioxide followed by lower alkanes and carbon monoxide formation in the polyols APR. The sugar APR displayed the opposite behavior increasing the selective to alkanes along with an important decrease in the hydrogen selectivity.

Sugars are highly reactive under hydrothermal conditions. The conversion of xylose APR was almost complete at every conditions. The polyols manifested different behaviors. Nevertheless an increase in the reactivity did not induce any improvement in the selectivity to hydrogen.

Different variable effects were observed during the substrates APR. The structure of the molecule, acidity and temperature had different impacts on the substrate reactivity and hydrogen selectivity. Nevertheless the compounds tested exhibited similar behavior during the process.

The alkane selectivity was different for each substrate tested. Polyols were characterized by a higher selectivity to methane and ethane. These compounds can be a result of hydrogenolysis in the C-O bonds for small chains as C1 and C2 as it is shown in Figure 44. However, longer substrates suffer first the cleavage of C-C bonds via decarbonylation or retro-aldol reactions.

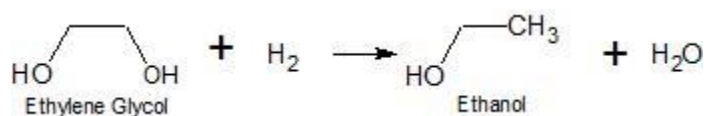


Figure 44 An example of C-O bond hydrogenolysis.

The sugar APR shows changes in the alkane selectivity with the temperature. At low temperature aldol condensation (i.e. Figure 45) and hydrogenolysis reaction could result in a higher selectivity to hexane and pentane.

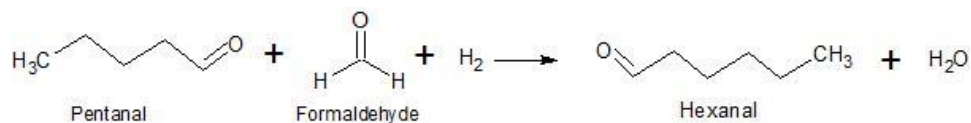


Figure 45 An example of aldol condensation.

Increase in acidity did not produce any changes in the alkane distribution for polyols but gave an important selectivity decrease for every alkane compound. Dehydrogenation reaction (i.e. Figure 46) followed by decarbonylation or retro-aldol reactions could be responsible for a decrease in the alkane production.

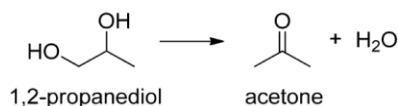


Figure 46 An example of dehydration reaction.

Xylose and formic acid APR produced a significant increase in the alkane production followed by changes in the final distribution. Due to aldol condensations between these substrates and reaction intermediates some of the alkane could be formed. Nevertheless the acidic conditions promoted hydro-dehydroxylation of xylose (Figure 47) confirmed by the presence of furfural in the liquid phase during the experiments with formic acid and xylose APR.

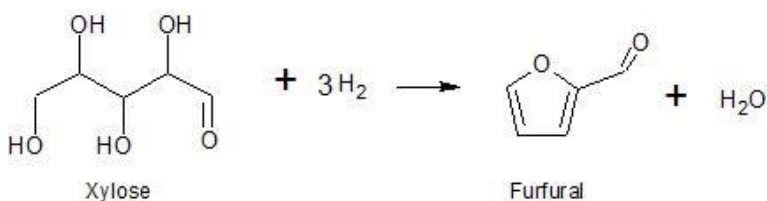


Figure 47 Xylose hydro-dehydroxylation.

The presence of liquid products as ethanol, propane diol, butane diol, etc. during different experiments is in line with the hypothesis of C-O bonds hydrogenolysis. However the presence of these molecules could be explained also by a dehydration reaction followed by reduction of carbonyl groups.

Presence of lactic, acetic, glycolic and other acids suggest the acid formation via water addition (Figure 48). Furthermore the acid production can be motivated by rearrangement of the molecules i.e. glyceraldehyde to lactic acid.

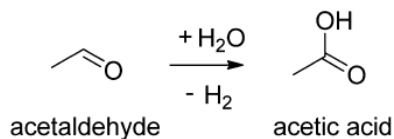


Figure 48 An example of acid formation.

Methanol and propane diols were the most important reaction products present in the liquid phase for every substrate and at all conditions. It is important to emphasize methanol as an intermediate in ethylene glycol APR according to the literature [15] while propane diol is an intermediate in glycerol APR [16].

Decarbonylation (Figure 49) and retro aldol reactions (Figure 50) were expected for the liquid products. However, the chains with even numbers of carbon had a trend to present most of their liquid intermediates in the carbon group with the half of their carbon number i.e. ethylene glycol APR went to C1, erythritol APR to C2 and sorbitol APR to C3. The odd compounds show a similar behavior but it was more complex to observe. Glycerol reacted to C1 and C2 molecules, while in xylitol and xylose APR the main liquid phase products were C2 and C3. These results define the retro aldol reactions as the main path for C-C cleavage.

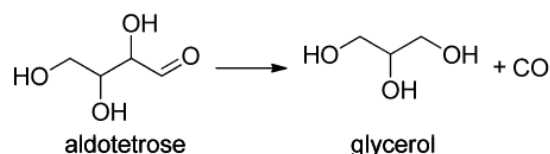


Figure 49 An example of decarbonylation reaction.

Decarbonylation reactions were observed based on the liquid phase products even if their contribution was not significant. These reactions could be responsible for production of alkanes.

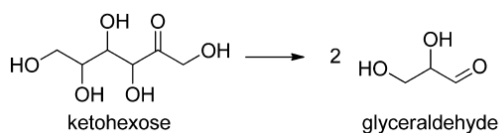


Figure 50 Example of retro-aldol reaction.

Longer products of aldol condensation were found in a low amount (ca. 5%) in the liquid phase and just in some experiments e.g. glycerol in ethylene glycol APR. Nevertheless in the gas phase production of longer molecules was observed in each experiment. Hence the aldol condensation had a higher probability to occur between reaction products of a smaller carbon chain.

Therefore the tested substrates exhibited the same set of reactions but the differences between them were related to the amount of intermediates and their nature (sugar or polyols). In any case C2 and C3 products were the most abundant for every substrate.

The carbon balance suggests a good identification of the main products for most of the substrates tested. Moreover most of the polyols displayed complete carbon identification. The gap in xylitol and xylose was identified to be related to furan chemistry during the liquid phase analysis.

The gas production seen to be temperature dependent and was improved by addition of formic acid. However, exact quantification of this effect is challenging because the gas production was dependent on the substrate.

Experimental errors were responsible for values exceeding 100% in the carbon identification in polyol APR. However, the error has never been more than 10% and the calibration was checked at the beginning and also at the end of the experimental part.

3 Kinetic modeling of ethylene glycol APR

The aim of this chapter is to report the work done in order to model kinetics of ethylene glycol aqueous phase reforming. This model was developed based on experiments at 3 different temperatures changing the residence time.

3.1 Mathematical modeling

The modeling started with a reaction pathway proposed for ethylene glycol APR (Appendix A). Most of the liquid phase intermediates can be neglected because of the low concentrations. The same is valid for alkanes and carbon monoxide in the gas phase. Thus a simplified reaction network was developed including just the major compounds identified in the experimental part. The scheme is given in the Figure 51. However other models were tested (Appendix B) until this description of the data was obtained.

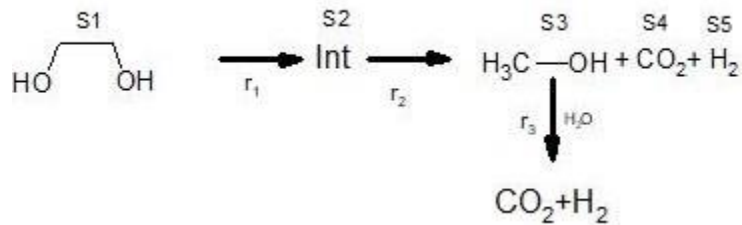
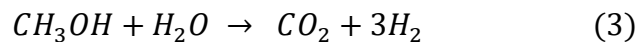
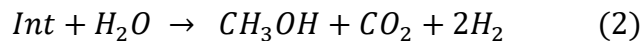


Figure 51 Aqueous phase reforming of ethylene glycol: main pathways selected for mathematical model.

Figure 51 shows the final model used for the ethylene glycol APR. This model is characterized by formation of an intermediate as the rate determining step for the production of methanol, CO₂ and H₂. In addition methanol can be decomposed into carbon dioxide and hydrogen.

The reactions balance for this model can be expressed as:



Where notation for reactants is shown in Figure 52.

The reaction rates were written as:

$$r_1 = k_1 * C_{S1} \quad (4)$$

$$r_2 = k_2 * C_{S2} \quad (5)$$

$$r_3 = k_3 * C_{S3} \quad (6)$$

Where:

- $r_1 - r_3$ are reaction rates.
- $k_1 - k_3$ are rate constants.
- $C_{S1} - C_{S3}$ are concentrations.

The rate constants were calculated as:

$$k_i = k_{0i} e^{-\frac{Ea_i}{R} \left(\frac{1}{T} - \frac{1}{T_{mean}} \right)} \quad (7)$$

Where T_{mean} is the average temperature of experiments.

Generation rates of compounds can be written as:

$$\frac{dC_{S1}}{d\tau} = -r_1 \quad (8)$$

$$\frac{dC_{S2}}{d\tau} = r_1 - r_2 \quad (9)$$

$$\frac{dC_{S3}}{d\tau} = r_2 - r_3 \quad (10)$$

$$\frac{dC_{S4}}{d\tau} = r_2 + r_3 \quad (11)$$

$$\frac{dC_{S5}}{d\tau} = 2r_2 + 3r_3 \quad (12)$$

Where τ is residence time.

3.2 Experiments

The setup used for these experiments was the same as in the experimental part. Ethylene glycol was pumped into the reactor as a 3 wt% aqueous solution. The catalyst was 2.5 wt% Pt and 1.25 wt% Pd supported on mesoporous carbon sunit. The liquid flow was changing through the experiments and the gas flow was constant. During the experiment three different temperatures were tested 200, 225 and 250°C. The pressure was always seven bars over the steam pressure. The utilized conditions are shown in Table 5.

Table 5 Conditions tested during ethylene glycol APR.

Experiment	Temperature	Liquid flow	N ₂ Flow	Pressure
n°	°C	ml/min	mol/min	bar
1	200	0.1	0.001472	24
2	200	0.2	0.001472	24
3	200	0.3	0.001472	24
4	200	0.4	0.001472	24
5	225	0.1	0.001472	32
6	225	0.2	0.001472	32
7	225	0.25	0.001472	32
8	225	0.3	0.001472	32
9	225	0.4	0.001472	32
10	250	0.1	0.001472	46
11	250	0.15	0.001472	46
12	250	0.2	0.001472	46
13	250	0.3	0.001472	46
14	250	0.4	0.001472	46

3.3 Results and discussion:

The kinetic model (eq. 4-12) was fitted to the experimental data (appendix C) by a combined Simplex - Levenberg - Marquardt method with an excellent explanation of the system. The sensitivity analysis of the results done with the Markov chain Monte Carlo method exhibited low uncertainty.

The calculated constants and the activation energies are given in Table 6:

Table 6 Calculated reaction constants and activation energies.

Reaction	Constant [s ⁻¹]		Activation energy [J/mol]	
	1	k ₁	1.76 * 10 ⁻²	Ea ₁
2	k ₂	5.86 * 10 ⁻⁷	Ea ₂	0.39 * 10 ⁵
3	k ₃	4.49 * 10 ⁻⁶	Ea ₃	0.24 * 10 ⁵

The error of estimation defined as:

$$R = \frac{(X_{exp} - X_{cal})^2}{(X_{exp} - X_{ave})^2} * 100\% \quad (23)$$

Where X_{exp} , X_{cal} and X_{ave} are respectively experimental, calculated and average flows (mol/min) values gave 99.56% goodness of the fit. Figures 52 to 56 illustrate excellent correspondence between the experimental data and the model estimation.

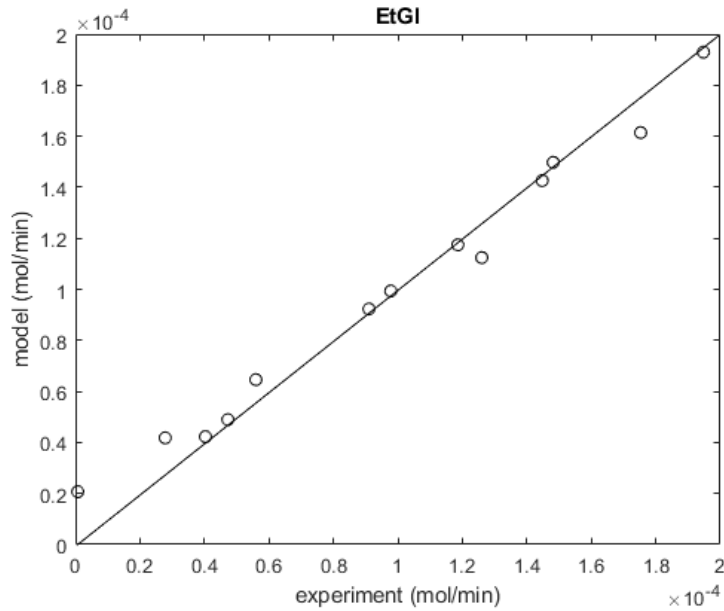


Figure 52 Ethylene glycol APR model vs experimental data.

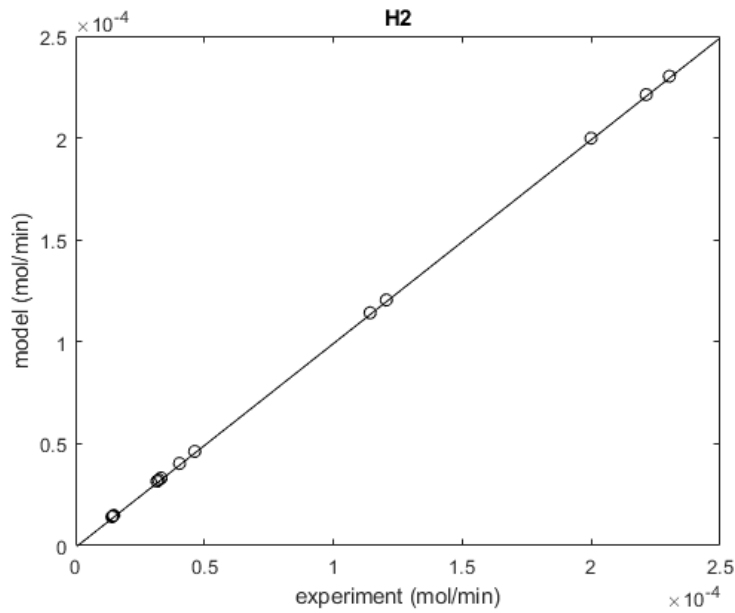


Figure 53 Hydrogen production model vs experimental data.

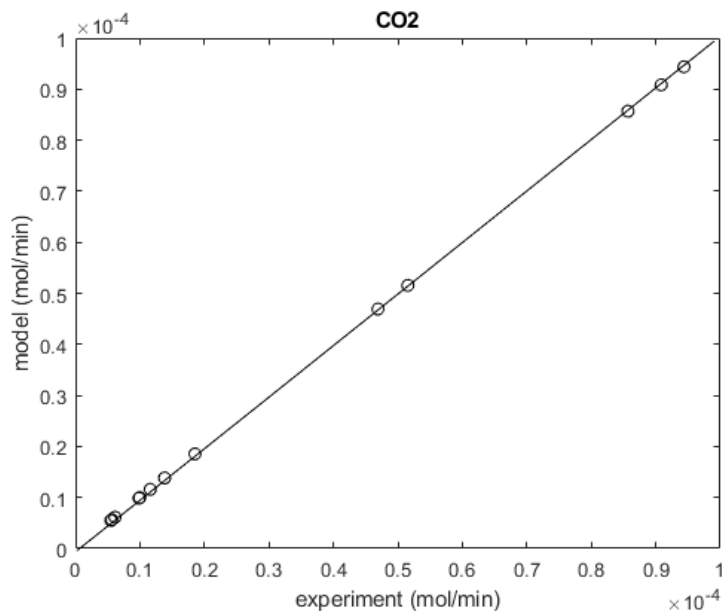


Figure 54 Carbon dioxide production model vs experimental data.

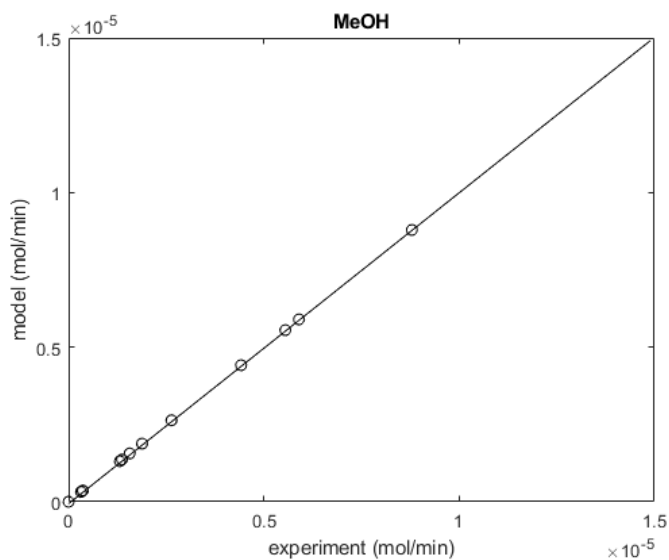


Figure 55 Methanol production model vs experimental data.

Results of sensitivity analysis are shown in appendix D. Figure D4 illustrates that the obtained constants are rather well defined. Nevertheless in the future the model can be further improved by addition of more intermediates and quantification of the adsorption terms.

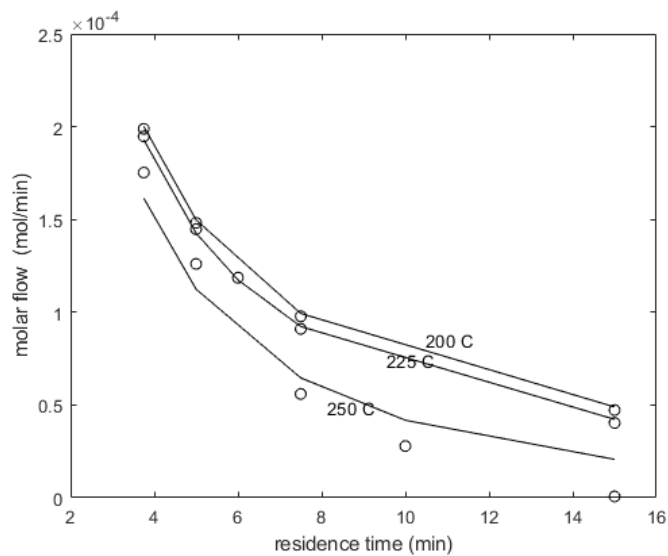


Figure 56 Ethylene glycol molar flow at the reactor outlet.

Behavior of the molar flow of ethylene glycol at the reactor outlet is shown in Figure 56 displaying a good agreement between the experimental data and calculations, which were done with the kinetic model, represented by eq. 4-6, 8-12, and the plug flow model.

4 Conclusions:

The aqueous phase reforming of five polyols and one sugar was done over a Pt/Pd catalyst. The experiments were performed in the temperature range of 175 to 225°C with a constant pressure of 32 bar. The gas phase was analyzed online in a micro-GC while the liquid samples were examined by HPLC. In total, 48 compounds were identified and quantified during the studies.

Polyols displayed a similar behavior which is highly selective to hydrogen and carbon dioxide. Moreover introduction of formic acid and temperature elevation had a positive impact on H₂ and CO₂ production. Xylose APR was different from xylitol displaying similar production of alkanes and hydrogen. Moreover presence of formic acid and higher temperature gave an increase in the alkane production making the process less selective to hydrogen.

Retro-aldol and decarbonylation reactions were identified as the C-C bond breaking reactions, retro-aldol reaction being the most prominent path.

Aldol condensation was the reason for formation of products with a carbon chain length exceeding the one for the substrate.

Hydrogenolysis of C-O bond and hydrogenation of carbonyl components are the main paths to most of the reaction products of the aqueous phase reforming. Thus it is necessary to ensure a low concentration of hydrogen in the liquid phase and a low partial pressure in order to decrease the amount of intermediates.

The presence of hydrogen in the liquid phase induces hydro-dehydroxylation of xylose, leading to furans and making production of alkane more favorable. Introduction of formic acid gave a rise in the aldol condensation reaction for sugars.

The liquid phase analysis pointed out a strong relation between the reaction paths. The molecules identified in the ethylene glycol and glycerol APR were helpful to recognize at least 75% of the total HPLC area in the other substrates. Moreover, the carbon balance was complete for most of the substrates.

The catalyst composition had an influence on selectivity to alkanes and carbon dioxide. The weight ratio between platinum and palladium gave the best results.

Kinetic modeling of ethylene glycol APR was done with goodness of fit of 99.56%. The model displayed an adequate correspondence between the experiments and calculations for all conditions. In the future quantification of more intermediates and addition of the adsorption terms could help to eliminate unknown intermediates in the model.

5 References

1. **R. Cortright, R. Davda, J. A. Dumesic**, *Hydrogen from catalytic reforming of biomass-derived hydrocarbons in liquid water*, *Nature*, 2002, Vol. 418, pp. 964-967.
2. **K. Murata, I. Takahara, M. Inaba**, *Propane formation by aqueous-phase reforming of glycerol over Pt/H-ZSM5 catalysts*, *Reaction Kinetics and Catalysis Letters*, 2008, Vol. 93, pp. 59-66.
3. **L. Godina**, *Aqueous-phase reforming of renewable polyols for sustainable hydrogen production*, PhD thesis, Abo Akademi University, 2019. pp. 4-6.
4. **A. Kirilin, A. Tokarev, H. Manyar, C. Hardacre, T. Salmi, J.P.Mikkola, D. Murzin**, *Aqueous phase reforming of xylitol over Pt-Re bimetallic catalyst: Effect of the Re addition*, *Catalysis Today*, 2013, pp. 97-107.
5. **N. Luo, K. Ouyang, F. Cao, T. Xiao**, *Hydrogen generation from liquid reforming of glycerin over Ni-Co bimetallic catalyst*, *Biomass and Bioenergy*, 2009, Vol. 34, pp. 489-495.
6. **J.A.Dumesic, J.W.Shabaker, D.A.Simonetti, R.D.Cortright**, *Sn-modified Ni catalysts for aqueous-phase reforming: Characterization and deactivation studies*, *Journal of Catalysis*, 2005, Vol. 231, pp. 67-76.
7. **A. Kirilin**, *Aqueous-phase reforming of renewables for selective hydrogen production in the presence of supported platinum catalysts*, PhD thesis, Abo Akademi University, 2013. p. 29.
8. **P. Claus, K. Lehnert**, *Influence of Pt particle size and support type on the aqueous-phase reforming of glycerol*, *Catalysis Communications*, 2008, Vol. 9, pp. 2543-2546.
9. **A. Kirilin, B. Hasse, A. Tokarev, L. Kustov, G. Baeva, G. Bragina, A. Stakheev, A. Rautio, T. Salmi, B. Etzold, J.P. Mikkola, D. Murzin**, *Aqueous-phase reforming of xylitol over Pt/C and Pt/TiO₂-CDC catalysts: catalyst characterization and catalytic performance*, *Catalysis science & technology*, 2014, Vol. 4, pp. 387-411.
10. **A.O.Menezes, M.T.Rodrigues, A. Zimmaro, L.E.P.Borges, M.A.Fraga**, *Production of renewable hydrogen from aqueous-phase reforming of glycerol over Pt catalysts supported on different oxides*, *Renewable Energy*, 2011, Vol. 36, pp. 595-599.
11. **G.Wen, Y. Xu, H. Ma, Z. Xu, Z. Tian**, *Production of hydrogen by aqueous-phase reforming of glycerol* 2008, *Hydrogen energy*, Vol. 33, pp. 57-66.

12. **M. Neira d'Angelo, V. Ordonsky, J. Van der Shaaf, J.C. Schouten, T. Nijhuis**, *Aqueous phase reforming in a microchannel reactor: The effect of mass transfer on hydrogen selectivity*, *Catalysis Science & Technology*, 2013, Vol. 3, pp. 2834-2842.
13. **R.R. Davda, J.W. Shabaker, G.W. Huber, R.D. Cortright, J.A. Dumesic**, *A review of catalytic issues and process conditions for renewable hydrogen and alkanes by aqueous-phase reforming of oxygenated hydrocarbons over supported metal catalysts*. *Applied Catalysis B: Environmental*, 2005, Vol. 56, pp. 171-186.
14. **J.W. Shabaker, G.W. Huber, R.R. Davda, R.D. Cortright, J.A. Dumesic**, *Aqueous-phase reforming of ethylene glycol over supported platinum catalysts*, *Catalysis letters*, 2003, Vol 83, pp. 1-8.
15. **J.W. Shabaker, J.A. Dumesic**, *Kinetics of aqueous-phase reforming of oxygenated hydrocarbons: Pt/Al₂O₃ and Sn-modified Ni catalysts*, *Industrial and Engineering Chemistry Research*, 2004, Vol 43, pp. 3105-3112.
16. **N. Luo, X. Fu, F. Cao, T. Xiao, P. P. Edwards**, *Glycerol aqueous phase reforming for hydrogen generation over Pt catalyst – Effect of catalyst composition and reaction conditions*. *Fuel*, 2008, Vol 87, pp. 3483-3489.
17. **L.I. Godina, A. V. Tokarev, I. L. Simakova, P. Mäki-Arvela, E. Kortesmäki, J. Gläsel, L. Kronberg, B. Etzold, D. Murzin**, *Aqueous-phase reforming of alcohols with three carbon atoms on carbon supported*, *Catalysis today*, 2018, Vol. 301, pp. 78-89.
18. **A. Wawrzetz, B. Peng, A. Hrabar, A. Jentys, A.A. Lemonidou, J.A. Lercher**. *Towards understanding the bifunctional hydrodeoxygenation and aqueous phase reforming of glycerol*, *Journal of Catalysis*, 2010, Vol. 269, pp. 411-420.
19. **D. L. King, L. Zhang, G. Xia, A. M. Karim, D. J. Heldebrant, X. Wang, T. Peterson, Y. Wang**, *Aqueous phase reforming of glycerol for hydrogen production over Pt–Re supported on carbon.*, *Applied Catalysis B*, 2010, Vol 99, pp. 206-213.
20. **L. I. Godina, A. V. Kirilin, A. V. Tokarev, I. L. Simakova and D. Yu. Murzin**, *Sibunit-supported mono- and bimetallic catalysts used in aqueous-phase reforming of xylitol*, *Industrial & Engineering Chemistry Research*, 2018, Vol. 57, pp. 2050-2067.
21. **A.V. Kirilin, B. Hasse, A.V. Tokarev, L. M. Kustov, G. N. Baeva, G.O. Bragina, A.Yu. Stakheev, A. Rautio, T. Salmi, B.J. M. Etzold, J.P. Mikkolaa and D. Yu. Murzin**, *Aqueous-phase reforming of xylitol over Pt/C and Pt/TiC-CDC catalysts: catalyst characterization and catalytic performance*, *Catalysis Science & Technology*, 2014, Vol. 4, pp. 387-401.
22. **A.V. Kirilin, A. V. Tokarev, H. Manyar, C. Hardacre, T. Salmi, J.P. Mikkolaa, D. Yu. Murzin**, *Aqueous phase reforming of xylitol over Pt-Re bimetallic catalyst: Effect of the Re addition*, *Catalyst Today*, 2014, Vol. 223, pp. 97-107.

23. **D. Yu. Murzin, S. Garcia, V. Russo, T. Kilpiö, L. I. Godina, A.V. Tokarev, A.V. Kirilin, I.L. Simakova, S. Poulston, D. Sladkovskiy, J. Wärna**, *Kinetics, modeling, and process design of hydrogen production by aqueous phase reforming of xylitol*, *Industrial & Engineering Chemistry Research*, 2017, Vol. 56, p. 13240–13253.
24. **A. Kirilin, J. Wärnä, A. Tokarev, D. Yu. Murzin**, *Kinetic modeling of sorbitol aqueous-phase reforming over Pt/Al₂O₃*, *Industrial & Engineering Chemistry Research*, 2014, Vol. 53, pp. 4580-4588.
25. **A. V. Kirilin, A. V. Tokarev, E. V. Murzina, L. M. Kustov, J.P. Mikkola, D. Yu. Murzin**, *Reaction products and transformations of intermediates in the aqueous-phase reforming of sorbitol*. *ChemSusChem*, 2010, Vol. 3, pp. 708-718.
26. **L. I. Godina, A. V. Kirilin, A. V. Tokarev, D. Yu. Murzin**, *Aqueous phase reforming of industrially relevant sugar alcohols with different chiralities*, *ACS Catalysis*, 2015, Vol. 5, pp. 2989-3005.
27. **R.R. Davda, J.W. Shabaker, G.W. Huber, R.D. Cortright, J.A. Dumesic**, *A review of catalytic issues and process conditions for renewable hydrogen and alkanes by aqueous-phase reforming of oxygenated hydrocarbons over supported metal catalysts*, *Applied Catalysis B*, 2005, Vol. 56, pp. 171-186.
28. **D. L. King, L. Zhang, G. Xia, A. M. Krim, D. J. Heldebrant, X. Wanga, T. Petersona, Y. Wang**, *Aqueous phase reforming of glycerol for hydrogen production over Pt–Re supported on carbon*, *Applied Catalysis B*, 2010, Vol. 99, pp. 206-213.

6 Appendix A

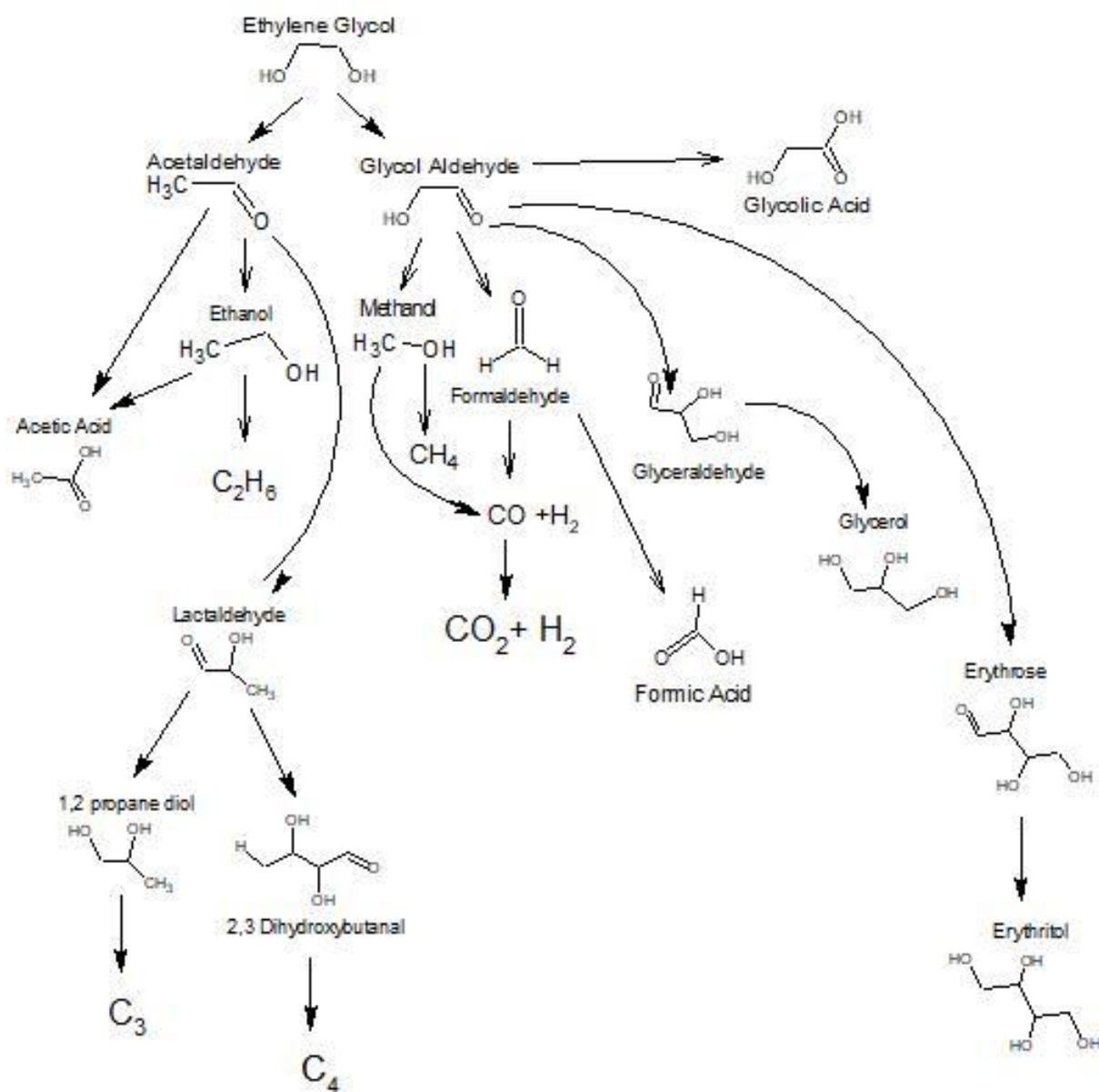


Figure A1 Complete reaction scheme of ethylene glycol APR.

7 Appendix B

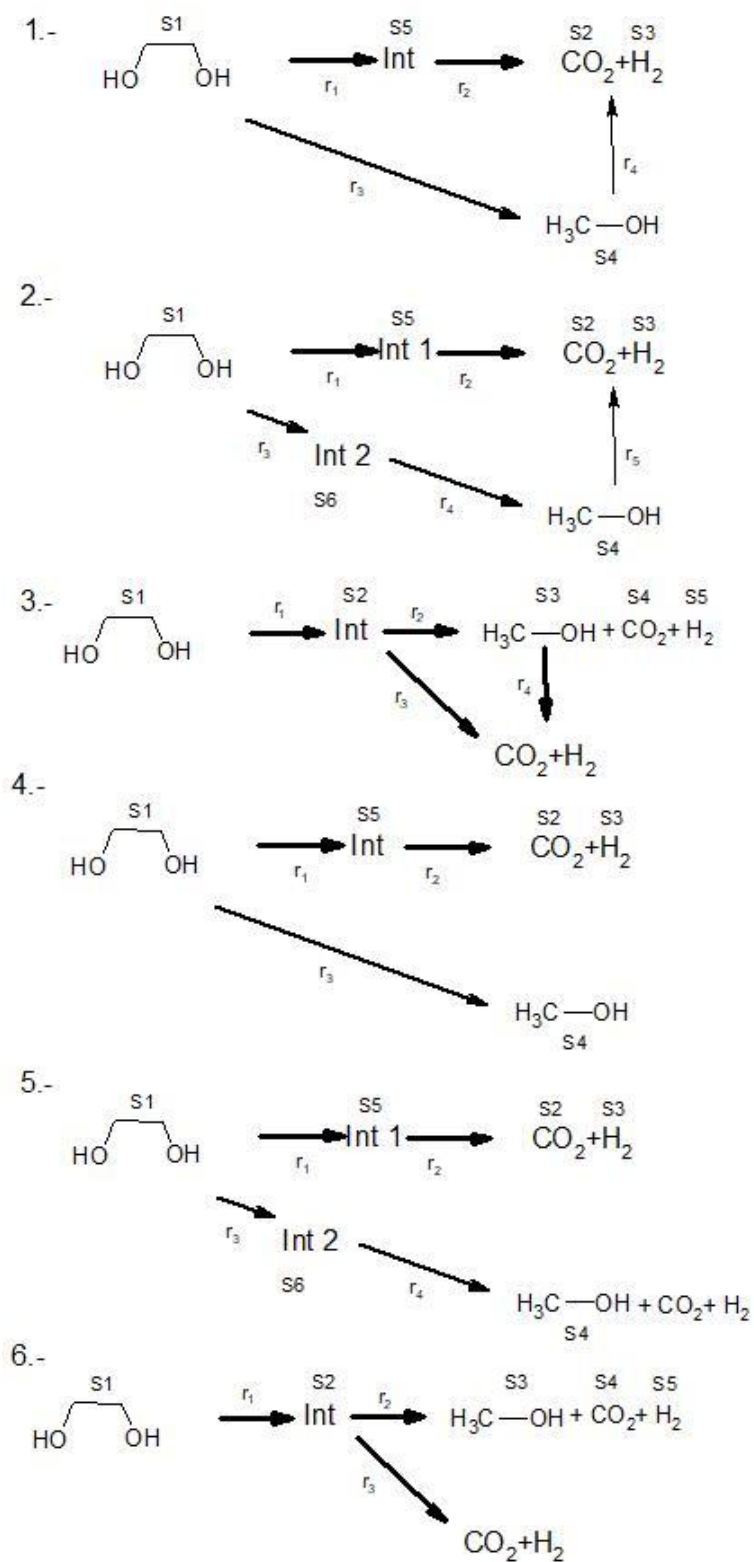


Figure B1 Reaction path tested for ethylene glycol modeling.

8 Appendix C

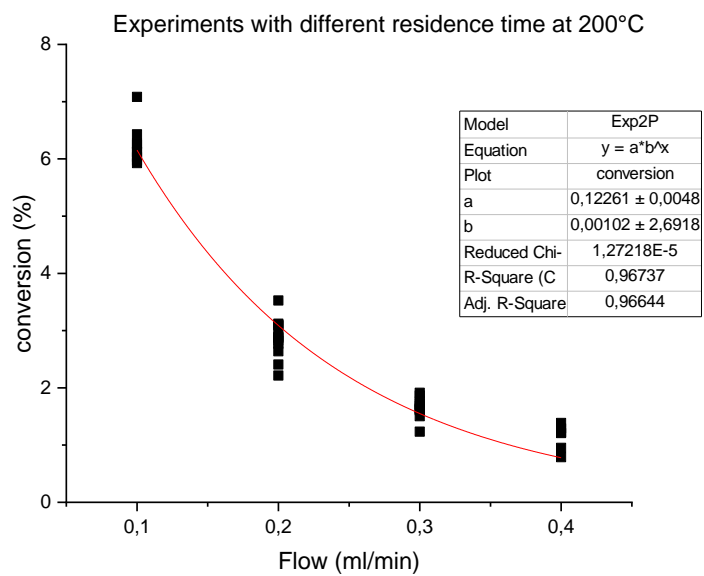


Figure C1 Conversion vs Flow at 200°C.

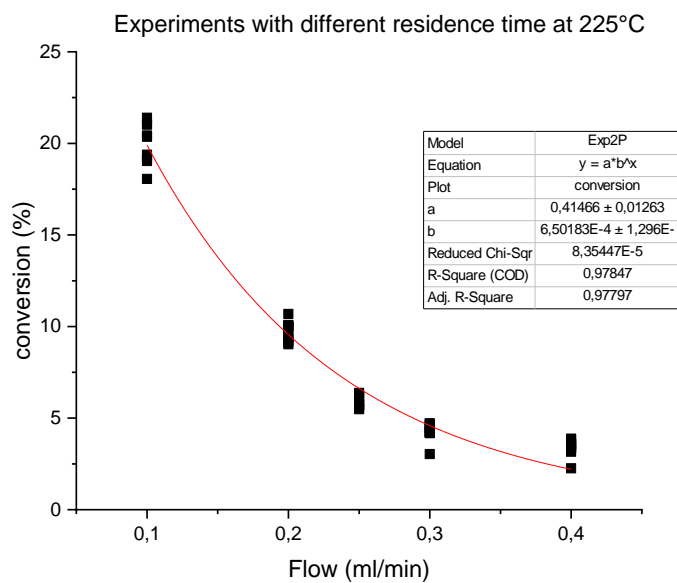


Figure C2 Conversion vs Flow at 225°C.

Experiments with different residence time at 250°C

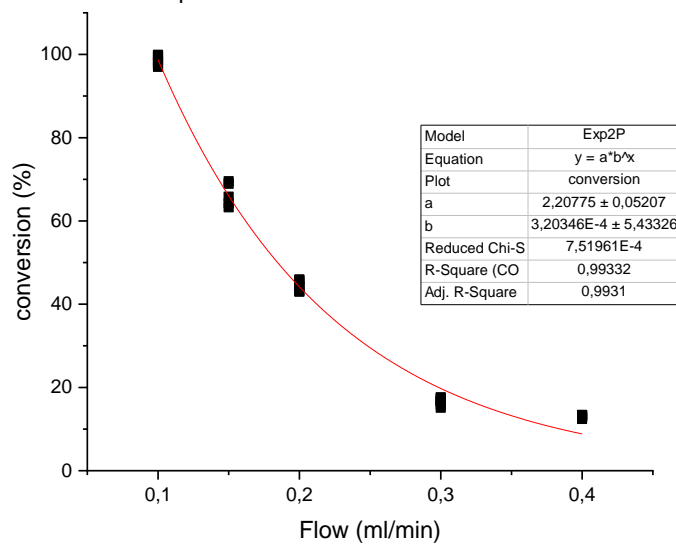


Figure C3 Conversion vs Flow at 250°C.

Table 7 Data used for ethylene glycol modeling.

Experiment	Temperature	Liquid flow	Gas Flow	Nitrogen Flow	Pressure	Residence time	Conversion	Catalyst	Ethylene glycol	H2	CO2	Methanol
									inlet	outlet	outlet	outlet
n°	°C	ml/min	ml/min	mol/min	bar	min	%	g	mol/min	mol/min	mol/min	mol/min
1	200	0.1	2.38	0.001472	24	14.95712262	6.24	0.5045	5.04064E-05	1.42286E-05	6.1354E-06	3.207E-07
2	200	0.2	2.38	0.001472	24	7.478561312	2.98	0.5045	0.000100813	1.41553E-05	5.51158E-06	3.5965E-07
3	200	0.3	2.38	0.001472	24	4.985707541	2.01	0.5045	0.000151219	1.46038E-05	5.6506E-06	3.636E-07
4	200	0.4	2.38	0.001472	24	3.739280656	1.38	0.5045	0.000201626	1.48485E-05	5.50416E-06	0
5	225	0.1	1.88	0.001472	32	14.95712262	19.98	0.5045	5.04064E-05	4.62365E-05	1.85345E-05	1.5654E-06
6	225	0.2	1.88	0.001472	32	7.478561312	9.72	0.5045	0.000100813	4.03571E-05	1.383E-05	2.6365E-06
7	225	0.25	1.88	0.001472	32	5.982849049	5.87	0.5045	0.000126016	3.16023E-05	1.16001E-05	1.31266E-06
8	225	0.3	1.88	0.001472	32	4.985707541	4.26	0.5045	0.000151219	3.22512E-05	9.85502E-06	1.3646E-06
9	225	0.4	1.88	0.001472	32	3.739280656	3.39	0.5045	0.000201626	3.31903E-05	9.97739E-06	1.8822E-06
10	250	0.1	1.37	0.001472	46	14.95712262	98.6	0.5045	5.04064E-05	0.000230278	9.43735E-05	2.63375E-06
11	250	0.15	1.37	0.001472	46	9.971415082	63.15	0.5045	7.56096E-05	0.000221267	9.0848E-05	8.79008E-06
12	250	0.2	1.37	0.001472	46	7.478561312	44.49	0.5045	0.000100813	0.000199901	8.56913E-05	4.4172E-06
13	250	0.3	1.37	0.001472	46	4.985707541	16.65	0.5045	0.000151219	0.000114244	4.69187E-05	5.5509E-06

14	250	0.4	1.37	0.0014 72	46	3.739280 656	13.05	0.504 5	0.000201 626	0.000120 534	5.1551 9E-05	5.8985 E-06
----	-----	-----	------	--------------	----	-----------------	-------	------------	-----------------	-----------------	-----------------	----------------

9 Appendix D

Table 8 Parameters with errors.

Constant	Estimated parameter	Estimated Std Error	Est. Relative Std Error (%)	Parameter / Std. Error
k1	1.76E-02	2.91E-03	16.5	6
k2	5.86E-07	3.41E-02	*****	0
k3	4.49E-06	6.00E-02	*****	0
Ea1	1.40E+05	1.49E+04	10.6	9.4
Ea2	3.92E+04	5.08E+09	*****	0
Ea3	2.44E+04	1.19E+09	*****	0

The correlation matrix of the parameters:

```

k1  1.000
k2  0.001  1.000
k3  -0.001 -0.717  1.000
Ea1 -0.958  0.011 -0.008  1.000
Ea2 -0.001 -0.992  0.711 -0.011  1.000
Ea3  0.001  0.700 -0.976  0.008 -0.713
      1.000
    
```

Sensitivity analysis:

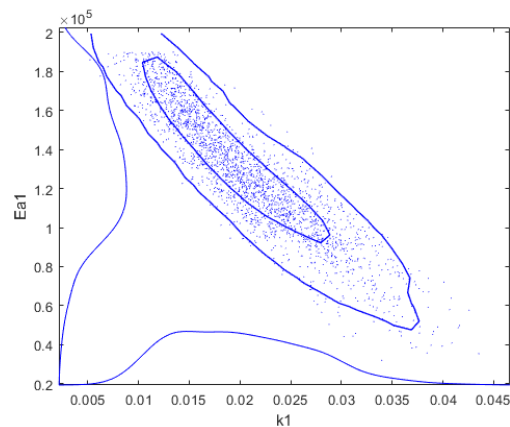


Figure D1 Ea1 vs k1.

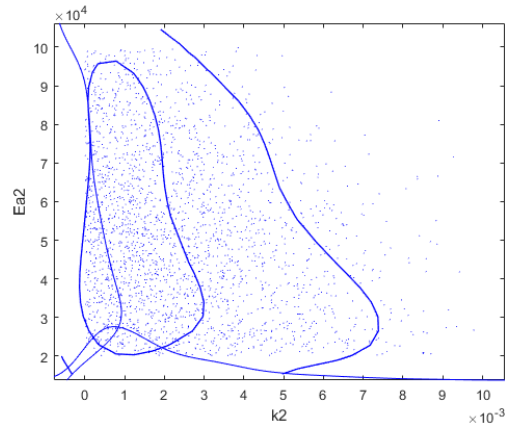


Figure D2 Ea_2 vs k_2 .

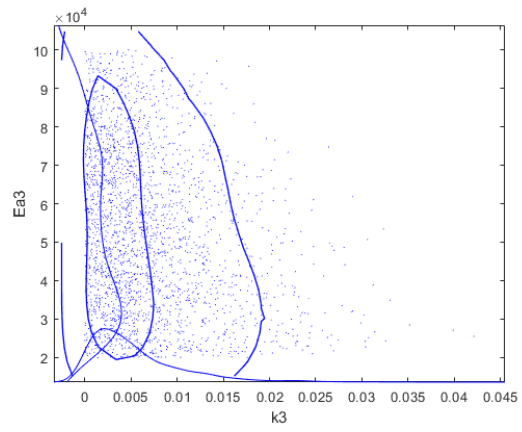


Figure D3 Ea_3 vs k_3 .

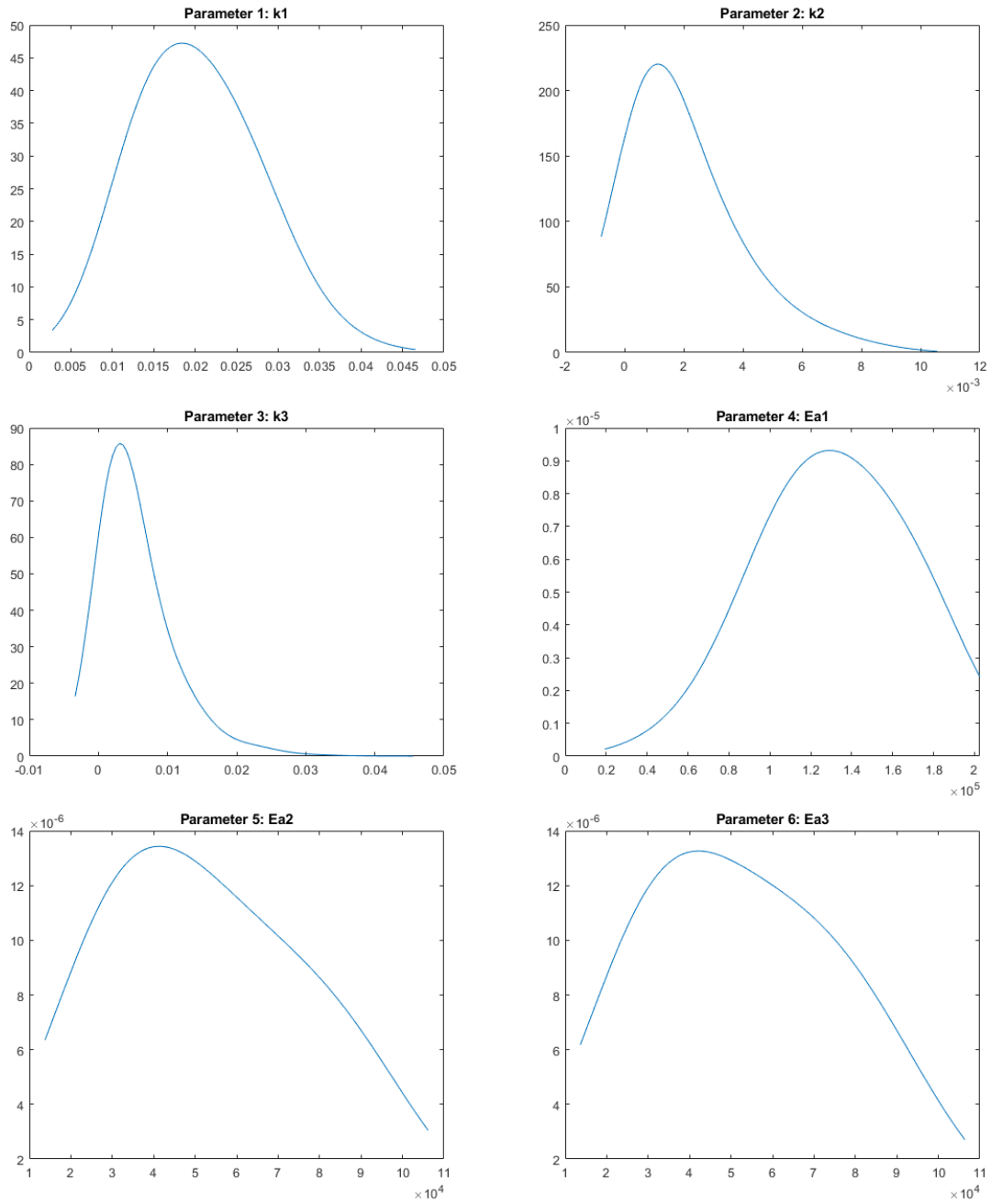


Figure D4 Sensitivity by parameter.